THE UNIVERSITY OF
SYDNEY

'VOR' - An Interactive iPad Model of the Combined Angular and Linear Vestibulo-ocular Reflex

Stephen Rogers

A thesis submitted in fulfilment of the requirements for the degree of Master of Science.

School of Psychology
Faculty of Science
University of Sydney

2015

Acknowledgements

I would like to thank Prof Ian Curthoys, Prof Iain McGregor, Dr Ann Burgess and especially Dr Hamish MacDougall of the School of Psychology, University of Sydney for their invaluable help, advice and encouragement during the preparation of this thesis.

Table of Contents

Table of Figures

1. Introduction

The purpose of the present thesis is to describe a simple model of the operation of the human vestibulo-ocular system developed in collaboration with Hamish MacDougall, and to implement the model in the form of a computer software application that runs on the Apple iPad.

The vestibular system consists of a bony labyrinth in the inner ear containing 5 sense end organs. Three end organs are associated with semicircular canals (SCC), of which each is maximally sensitive to angular accelerations of the head around one of 3 approximately orthogonal axes. Two end organs (the so-called *otolith organs*) are each maximally sensitive to linear accelerations of the head in one of 2 approximately orthogonal planes. The otolith organs are the utricular macula, which lies approximately in the horizontal plane, and the saccular macula, which lies approximately in a vertical plane. Six degrees of freedom (DOF) are required to specify motion and acceleration in all directions, and this combination of canals and otoliths is sufficient to sense these linear and angular accelerations of the head.

Afferent inputs from the vestibular end organs contribute to balance, proprioception and vision. In particular, the vestibulo-ocular reflex (VOR) produces oculomotor responses in a direction opposite to head movement and tend to stabilise visual images on the retina.

In general terms, a scientific model represents a simplified view of a complex natural system and contains conceptual elements analogous to real structures and processes. The validity of a model is the degree to which the behaviour of the model, and in particular its predictions, match real world observations. The present model provides

conceptual elements analogous to sensory end organs, sensory and motor neurons, a conceptual "vestibular nucleus" and eye muscles. The model makes a series of assumptions about the processes that underlie the real VOR, and these assumptions are clearly expressed as part of the definition of the model.

The mechanisms by which head movements are detected in the end organs in the labyrinths of the inner ear are well understood, and there is wide agreement about many forms of observed eye movements driven by afferent signals from these end organs. Research into neuronal anatomy has partially mapped the projections from the end organs via the vestibular nuclei to the extra-ocular muscles. But there remains a need for a more complete theoretical description of the processes by which afferent inputs are converted into motor outputs. The goal of the present work is to implement a model of these processes. The success of the model will depend on the degree to which it predicts eye movement responses driven by head movement stimuli where the eye movements have been observed in real human subjects under similar conditions.

Research into the operation of the human vestibular system has largely been conducted using whole body motion equipment, whereby a subject is securely attached to an apparatus that allows rotation around, and sometimes linear movement along, one or more axes. The subject is fitted with some form of device that accurately detects eye movements. Traditionally scleral search coils embedded in an object similar to a contact lens have been placed in direct contact with the eye, allowing precise changes in eye orientation to be detected by changes in current flowing through the coils induced by a magnetic field. Although providing accurate measurements, the scleral coil devices are uncomfortable for the subject and require

that the subject be located within a frame containing transmitter coils. Recently video recording has been used, whereby eye position is determined by processing a video image to detect the horizontal and vertical location of the pupil, and iral landmarks for torsion. Such video cameras must be fixed relative to the head, and recent advances in technology have allowed very small cameras to be attached to goggles, which are firmly attached to the subject's face. This provides maximum flexibility of movement of the head, allowing the recording of eye movement during rapid accelerations such as those during the head impulse test (Halmagyi & Curthoys, 1988), and the system may be transported to any convenient location for making observations.

During typical vestibular tests the subject is instructed to fixate upon a point relative either to their head or to the world. For example, when the subject is placed on a rotating chair and accelerated angularly over some duration the fixation point is fixed relative to the chair and head. This scenario challenges the subject to suppress the VOR in order to maintain fixation. Conversely, when conducting a head impulse test the fixation point is usually fixed relative to the world. This scenario allows measurement of the effectiveness of the VOR, which in a normal subject will drive the eyes to maintain fixation on the earth-fixed target during the rotation of the head.

The model described here is presented in the form of a software application, which can be programmed with motion profiles to be applied to a virtual subject, represented as the surface of a head graphically displayed on the device screen. The mechanical effects of the kinematics of these motion profiles are calculated at the location of the labyrinths in each side of the head in terms of linear and angular accelerations. The model converts these accelerations into notional afferent neuron signals and uses these signals as inputs into an internal representation of head position (RHP). Outputs

from the RHP are interpreted to produce motor signals to the eye muscles and the resulting eye movements are displayed as part of the head on the screen. Imaginary lines of sight are drawn on the screen to clarify the eye movements. Afferent inputs, motor outputs and intermediate elements of the calculations are available to be graphed on the device screen.

The goal of the present work is to describe a model that predicts eye movements similar to those that would be observed in a real human subject undergoing the stimuli defined by the various motion profiles. Various conditions can be applied to the subject, such as neuronal or labyrinthine dysfunction, and the model predicts the effects of these conditions.

It is important to note that some parts of the present model describe structures or processes which have not in fact been measured or detected in real human subjects. This is not considered a valid objection to the model. It may be that such structures and processes may yet be discovered in reality. It is hoped that as the model is distributed and examined it will suggest the existence of hitherto unknown mechanisms, which can then be searched for in real subjects.

There are many models of vestibular function proposed in the literature. A lot of these use classic "box and arrow" diagrams to explain complex interactions between vaguely defined modules and algorithms. Some of these are quite focused with a narrow scope without much consideration for consistency or compatibility with other aspects of vestibular function.

The broad model implemented in this project is different in that it attempts to construct a functional and internally consistent algorithm for a simple "bionic" VOR

able to produce idealised but biologically plausible eye movement responses to a huge range of interactive motion stimuli.

In order to attempt to construct such a bionic VOR we needed to collapse a great deal of complexity down to a small number of assumptions derived from observation, first principles, and the practical demands of a model that works in real time and in response to a wide range of linear and angular movement stimuli.

The model does not simply attempt to replicate a limited set of observations but is generic enough to make predictions about the eye movement response to almost any stimulus that can be imagined by the researcher, without the tuning or adjustment of variables typically employed to align model predictions with new observations.

The extent to which the modelled eye movement responses of the *VOR* app match existing observations, and predict future observations, will indicate to what extent the simplified model is useful for understanding the far more complex vestibular function of real organisms, identifying which features of the many vestibular models are absolutely necessary for a functional bionic VOR and reconciling inconsistencies and contradictions in our conception of various features of the VOR.

This strategy also aims to provide the beginnings of a framework on which systematically to build additional modules including those that allow other sources of motion stimuli (device motion, motion replayed from file, remote control etc.), artificial stimuli (caloric irrigation, galvanic stimulation, pressure, vibration etc.) and visualisation and manipulation of individual afferent populations (regular, irregular etc.). Such a framework provides a roadmap, discipline and tests of internal consistency because all the modules need to work together.

The eye movement predictions from the *VOR* app will almost certainly differ from the observations and expectations of various researchers, but if we succeed in provoking (and hopefully resolving) some of these disagreements then one of the main aims of the project will have been met.

2. aVOR

In February 2012 *aVOR* was released for free download on the Apple iTunes Store. *aVOR* (derived from *angular vestibulo-ocular reflex*) was the implementation of a model developed with Hamish MacDougall. *aVOR* makes use of certain innovative hardware features of the Apple iPhone - namely, the touchscreen, high-resolution graphic display, linear accelerometers and gyroscope - to present an interactive model of some aspects of the functional human vestibular system, including the simulation of some kinds of labyrinthine and cerebral disorder.

aVOR displays a 3-dimensional surface of a human head, including eyes and bilateral vestibular labyrinths. The labyrinths are usually displayed at a greatly enlarged scale so that details of canal activation and inhibition, and the drift of otoconia characteristic of canalithiasis, causing benign paroxysmal positional vertigo (BPPV), can be seen clearly on the screen. (Otoconia are dense calcium carbonate crystals suspended in a gelatinous layer attached to the otoliths, providing part of the mechanism which responds to linear accelerations. BPPV can occur when otoconia become detached from the otoliths and drift freely in the endolymph contained by the semicircular canals, creating pressure changes which are interpreted neurally as angular acceleration.) Horizontal, vertical and torsion eye movements are driven by the simulated activation and inhibition of the semicircular canals, which in turn are calculated based on rotations of the head and the drift of otoconia caused by gravity. The app provides the facility to simulate end organ dysfunction in any of the semicircular canals, and the presence of free otoconia. Such characteristics affect the simulated activation/inhibition of the canals.

In *aVOR* model eye movements were driven solely by a combination of canal activation and a simulated drift towards a fixation point (fixed relative to either the head or the world) at a limited rate: nominally 20°/sec. A saccade (rapid eye movement to bring the gaze to fixation target) is triggered whenever the angle between eye direction and fixation target exceeds a certain value, nominally 10 degrees. A delay is inserted between the saccade trigger and its occurrence. The delay may be adjusted to simulate covert (with a delay between trigger and saccade of a nominal 20ms) and overt (100ms) saccades, or extended (500ms) to enhance saccade visibility in the app. Disabling the drift towards target entirely, and instead inserting regular saccades towards the fixation point (nominally at 5 Hz) simulated cerebellar dysfunction. This was a gross over-simplification of the effect of cerebellar dysfunction; in reality there is always slow phase eye movement preceding quick phases, but the setting was included to remind operators that many conditions can cause VOR dysfunction.

Head rotation and orientation are determined in *aVOR* both by touch gestures on the screen, which are used to manipulate the model of the head, and also by the orientation and motion of the device itself. Head rotation stimulates the canals, and head orientation determines the direction of gravity, which is used to calculate the position of any freely drifting otoconia. Canal activation is calculated using angular velocity as a simple approximation of the leaky integration of angular acceleration, and drives activation or inhibition at a nominal firing rate of 2.0 spikes per degree per second, added to or subtracted from the resting rate, nominally 150 Hz. This activation, in turn, drives eye direction and torsion with a gain of 1.0 for normal function and 0.0 for dysfunction. Finally, dysfunction may be defined as acute or compensated. In an "acute" patient the pathological reduction in firing rate from the

normal resting rate produces a central response that is similar to an inhibitory stimulus that produces slow phase eye velocity and therefore spontaneous nystagmus (a condition consisting of a series of involuntary eye movements caused by afferent signals from the vestibular end organs which are incongruent with head movement). In a "compensated" patient this reduction in spontaneous firing rate had become the new norm, such that it is no longer interpreted as an inhibitory stimulus and does not produce nystagmus.

3. VOR

Up to August 2014 *aVOR* had been downloaded to more than 23,000 Apple devices in 100 countries, has been well received and is very highly regarded as a teaching tool. Every App Store rating scored 5 stars out of 5. However, for pragmatic reasons it simplified the vestibulo-ocular system in several significant ways. The objective of the present study was to implement the development of a new and more sophisticated tablet application - *VOR* - that extends the functionality of *aVOR*. The *VOR* model was developed in collaboration with Hamish MacDougall and this thesis aims to describe and implement that model. *VOR* was designed to be a research tool rather than just a simplified teaching aid. It takes a more sophisticated approach to the interaction between end organ afferents, vestibular nuclei and the control of eye movements. *VOR* attempts to implement the simplest model of the VOR that is able to demonstrate ocular behaviour similar to established empirical observations, and predicts responses to situations and conditions that have yet to be tested. *VOR* attempts to simplify and collapse many complex functions into the most minimal components required to capture a first approximation of the VOR that can easily be understood and implemented. The extent to which the app's predicted responses match current and future actual observations will help to identify which of the many complex, esoteric, and sometimes contradictory mechanisms referred to in the mountain of vestibular literature are absolutely necessary to a functional bionic model of the VOR. The interactive nature of the app will make it accessible to researchers and students worldwide and provide a common platform allowing the sharing of theoretical developments and empirical observations.

In general terms, the addition of the following features and aspects of the vestibulo-ocular system distinguish *VOR* from *aVOR*:

1. Researcher-programmable motion profiles consisting of sequences of linear and angular transforms of a device able to move a virtual subject relative to the world, and of the subject's head relative to the device.

   VOR includes a predefined series of motion profiles, such as forward- and backward-facing centrifugation, sinusoidal rotation and off-vertical axis rotation (OVAR). *VOR* also provides the researcher with the ability to experiment by adjusting these profiles and creating new combinations and sequences of rotations and translations. These profiles can be exchanged between researchers, for example by email, and reproduced by the app on different devices, thus providing the opportunity to share and compare observations and theories. This will greatly facilitate the development of new experiments to test vestibular function.

2. Researcher-programmable end organ conditions.

   Certain disease states are associated with changes in the gains and resting firing rates of the signals from various end organs. *VOR* includes a range of basic conditions and the pattern of effects they have on end organ function. For example, unilateral superior neuritis is programmed to reduce the gains and resting rates of the anterior canal, lateral canal and utricle of one labyrinth by 70%. *VOR* provides the researcher with the ability to experiment by

adjusting the effects of these conditions and to define new conditions by specifying the relative gains and resting rates of various end organs individually. Again, these definitions can be exchanged between researchers and incorporated into the app on different devices.

3. Semicircular canal activation driven by acceleration, not velocity.

aVOR's first approximation of canal activation was driven by angular velocity as the simplest implementation needed, because the app limited manipulation of the head to small rotations of no more than about 90 degrees. These rotations were also transient so that adaptation to the rotation was negligible.

Through its researcher-programmable motion device-based tests *VOR* can model sustained linear and angular velocities and accelerations. In these circumstances it is more appropriate to implement a "leaky velocity integrator", which is supplied by signals from the acceleration-sensitive sensory hair cells of the ampullary cupulae, rather than directly from the angular velocity of the canals. Adaptation to these sustained stimuli is also included in the model.

4. The linear VOR.

VOR models afferent sensory input from the utricular and saccular maculae, which are sensitive to linear acceleration of the head and are known to make a

contribution to the VOR. Linear acceleration of the head gives rise to an ocular response in the direction opposite to acceleration. The magnitude of this response is approximately inversely proportional to the fixation distance.

5. The contribution of the otoliths to the angular VOR.

Additionally, otolith input can drive *angular* VOR. This can be observed, for example, during constant OVAR, where canal input decays to zero as the response to constant velocity rotation decays, but the steady influence of a modulating gravito-inertial acceleration (GIA) vector on the otoliths can drive steady horizontal nystagmus.

Under normal circumstances the angular information derived from canal and otolith input will tend to agree, and can be interpreted by the vestibular nuclei as having the same axis, direction and rate of rotation. Constant rotation around the vertical axis gives rise to lateral nystagmus, but this decays as the canals' response to constant velocity rotation decays. If the head angular velocity is then sharply reduced, nystagmus can be observed. In this example the horizontal canal adapts to steady angular velocity around the vertical axis, and subsequent deceleration of the head is interpreted as acceleration in the opposite direction. This incongruency gives rise to nystagmus.

If during the post-rotating nystagmus the head is tilted such that the head vertical axis is no longer vertical relative to the world, sensory input from the otoliths no longer agrees with input from the canals. It is observed that the

lateral nystagmus caused by angular deceleration abruptly ceases. This phenomenon is known as "tilt dumping". It is reasonable to assume that this is caused by a mismatch between the otolith and canal input, and that the vestibular nuclei corrects the estimation of head rotation by putting greater confidence in otolith input than canal input. A useful model of the vestibulo-ocular system, incorporating both canal and otolith input, should reflect this phenomenon.

4. Kinematics

The app maintains 3 frames of reference nested within each other: world, chair and head. Each can maintain a location, orientation, linear and angular velocities and accelerations. In addition, a fixation point can maintain a location, linear velocity and acceleration relative to the world, chair or head. The motion of each of the 3 frames and fixation position can be programmed using the app.

Locations are recorded as 3-dimensional vectors representing a location in space. Units are metres. The standard Hixson et al (1966) convention was adopted for labelling of axes: x for the naso-occipital axis, positive forward; y for the interaural axis, positive to the left from the subject's point of view; z for the vertical axis, positive upward.

Orientations are recorded as Hamiltonian quaternions. These can be interpreted as a series of three Euler rotations around the x, y, and z axes. The order of these rotations is according to the Fick convention: rotation around z axis (corresponding to horizontal eye movement) followed by rotation around the y axis (vertical eye movement) followed by rotation around the x axis (torsional eye movement). Rotations are defined according to the right-hand rule. Thus positive rotations around the z axis move to the left (from the subject's point of view), positive rotations around the y axis move downward and positive x rotations move clockwise (from the subject's point of view). Quaternions offer the advantage that they may be manipulated without regard to the singularities that appear in the Euler system near the x, y and z axes.

Linear velocities and accelerations are recorded as 3-dimensional vectors representing velocity or acceleration along the x, y and z axes in metres per second and metres per second squared respectively. Angular velocities and accelerations are recorded as 3-dimensional pseudo-vectors representing angular velocity or acceleration around the x, y and z axes in degrees per second and degrees per second squared respectively.

This system for representing the state of the world, chair, head and fixation point frames provides a convenient and consistent method for calculating kinematics and the resultant forces operating on the end organs. The world frame is statically located at the origin with unitary orientation and is subject to a constant linear acceleration due to gravity at 9.81 m/s in the positive direction along the z axis - ie. upwards. The state of the chair frame is defined relative to the world frame and may have non-zero location, orientation, linear and angular velocities and accelerations. Likewise the state of the head frame is defined relative to the chair frame.

The state of each frame relative to the world is given by an iterative calculation based on the frame state and the frame's parent state (for the head, the parent is the chair; for the chair, the parent is the world) where:

orientation = parent orientation * frame orientation

velocity = frame orientation inverted
* (parent velocity
+ parent rotational velocity at frame)
+ frame velocity

acceleration = frame orientation inverted
* (parent acceleration

+ parent rotational acceleration at frame)

+ frame acceleration

gravity = frame orientation inverted * parent gravity

angular velocity = parent orientation inverted

* parent angular velocity

+ frame angular velocity

angular acceleration =

parent orientation inverted

* parent angular acceleration

+ frame angular acceleration

and

parent rotational velocity at frame =

parent angular velocity

× frame location

parent rotational acceleration at frame =

centripetal acceleration

+ tangential acceleration

and

centripetal acceleration =

parent angular velocity

× parent angular velocity

× frame location

tangential acceleration =

parent angular acceleration

× frame location

where * represents scalar, or matrix, or matrix-vector multiplication, and × represents the vector cross product.

All changes to a frame's position, orientation or derivatives of these take the form of a cosine function offset by 270° and are defined by the order of derivative of location or orientation with respect to time, the magnitude and the duration of the change. Sinusoidal (cyclic) changes to displacement, orientation, velocity etc. are defined by these parameters plus the frequency of the sinusoidal curve.

The following calculation is performed to determine the frame's position, velocity, acceleration etc. at each moment. d_1 represents the derivative which was specified in the change definition (0=change in displacement; 1=change in velocity etc.). d_2 represents the derivative which is to be calculated for the frame at time t (0=position; 1=velocity etc.).

Given

d_1 = derivative defined for the change

d_2 = derivative to be calculated for the frame at time t

t = time

f = frequency

a = amplitude

x = frame derivative d_2 (0=position etc.) at time t

if $d_2 > d_1$

$$x = a \sin(2ft\pi + (d_2-d_1-1)\pi/2) (2f\pi)^{d2-d1} / 2$$

if $d_2 <= d_1$

$$x = a \sin(2ft\pi + (d_2-d_1-1)\pi/2) (2f\pi)^{d2-d1} (2ft\pi)^{d1-d2} / 2(d_1 - d_2)!$$

5. Researcher-programmable Conditions Affecting End Organ Afferent Signals

In the present model normal subjects are characterised by canal responses (gain and resting rate) with a VOR gain of 1, and otolith responses with a VOR gain of 0.5. In practice a researcher could adjust these gain values to mimic any desired gain and resting rate values. The gain from any particular end organ, or set of end organs, can be adjusted by the application of a researcher-programmable set of end organ gain and resting rate values, which can be manipulated within the app and stored in the iTunes File Sharing area. Each condition is defined by a list of end organs, and a factor by which the gain and resting rate from that organ is multiplied before being submitted to the VOR calculation.

6. VOR Gain and the Representation of Head Position (RHP)

Our development of the *VOR* model underwent a profound change of direction during the development process.

The *aVOR* model detected changes in angular position (velocity) with the canals and translated these into equal and opposite changes in eye position (velocity) such that when the gain was 1.0, the eyes would perfectly compensate for head rotation. The mathematics involved was simple, particularly in that only a single eye position calculation was necessary, since the gaze directions from the eyes were always parallel.

Our initial approach was to retain this angular contribution to the VOR, and to simply add the linear component based on the otolith afferents. The gain to be applied to this contribution would be dependent on the distance from the head to the fixation point. The fixation distance was determined based on the degree of ocular convergence.

In practice this method was inadequate for the task of predicting binocular eye movements based on complex angular and linear components of head movements.

Even considering only angular components of motion, the eye movements required to maintain gaze on a world-fixed point are disconjugate (different for each eye) and depend on (a) the distance between the head and the fixation point; (b) the fixation point angle offset from the primary position; and (c) the displacement of each eye relative to the centre of the head (see Figure 1). These dependencies are illustrated by a profile in which the fixation point is initially coincident with the primary position and 0.2m in front of the head (Section 13.2). At the moment of peak velocity during

this profile the head velocity is 200°/sec, the left eye velocity is 265°/sec and the right eye velocity is 289°/sec.

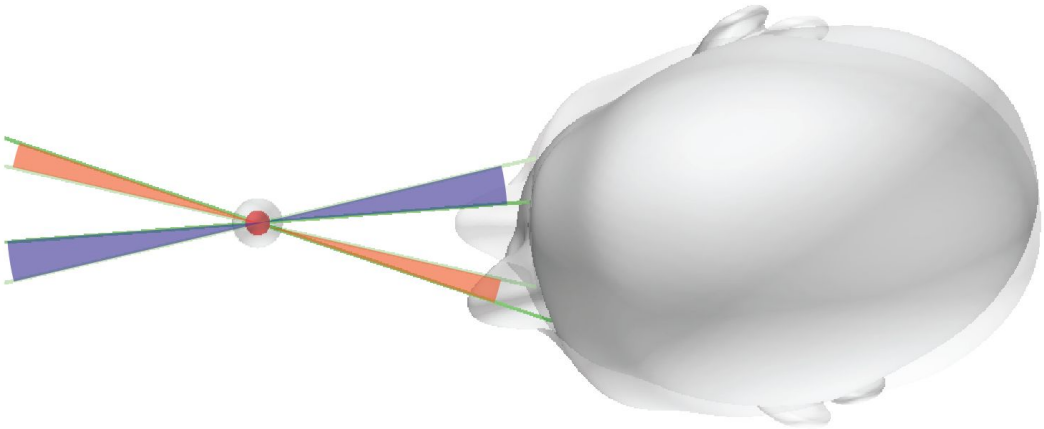

Figure 1. Disconjugate eye movements during head rotation with close fixation point

The calculation of linear components of VOR is significantly more complex. It is apparent that linear VOR is approximately inversely proportional to the fixation distance, but depends also on the fixation offset from the primary position and linear separation of the eyes.

It is of course possible to design formulae expressing the relationship between detected head movement and ocular responses in terms of trigonometry and calculus. These formulae could then be applied *forward-kinematically* to predict eye position and velocity in response to specific head movements in 6 DOF.

Approaching the issue from a different direction, we propose the following assumption: that a theoretically perfect vestibular system, developed through evolution and organic experiential feedback, would be wired such that all head movements relayed by the vestibular end organs will reflexively cause ocular

responses which maintain gaze on a world-static reference point (subject to oculomotor limits). According to this assumption, a hypothetical internal neural representation of world-referenced head position is constantly updated by afferent signals from the vestibular end organs, and through motor neuronal connections drives compensatory eye movements to maintain gaze.

We emphasise that this representation of head position (RHP) is purely a theoretical construct. We do not suggest that it might necessarily be objectively observed in practice, or even in principle. Instead we suggest it is literally a neural network, which like an artificial neural network in the field of information technology produces (oculomotor) outputs in response to (end organ sensory) inputs without explicitly specifying the rules by which this process is carried out. It is well known that artificial neural networks can be "trained" to carry out such functions through a process of unsupervised learning for which, arguably, there has been ample opportunity through both evolution and the experience of the individual organism.

Proceeding from the assumption that the theoretical RHP system is an appropriate and useful perspective on the VOR, we built a software model that converted angular acceleration around each canal axis as a scalar value and linear acceleration across each otolith plane as a vector lying in a simplified plane of the otolith.

Then change in RHP angular position was integrated from the sum of products of the scalar values for each canal and its respective axis. Change in RHP linear position was slightly more complicated: since otolith response to acceleration of a given magnitude along a given vector in 3 dimensions was limited to a shear vector across the surface of each otolith, converting otolith response back into the stimulus acceleration required multiplication by a 3x3 matrix representing the inverse of the

matrix which represents the sum of the saccular and utricular normal vector crosses, as described in *Otolith Contributions to the VOR Model* (Section 11). The combination of the angular and linear contributions to the change in head position provided precise updates to the RHP in 6 DOF.

Then the model performs the much simpler *reverse kinematic* calculations of eye position from the static world-referenced fixation point to the RHP. Eye positions are differentiated to calculate eye velocities.

Thus the model does not need to make assumptions about angular and linear VOR gains for fixation at various distances from the head and angles offset from the primary position - it need merely maintain a theoretical RHP and assume that gaze is perfectly maintained through any combination of angular and linear motion.

Experimental observations of real human VOR suggest that whereas eye movement response compensates accurately for angular head motion, response to linear head motion is somewhat attenuated. Our model accommodates this by simply attenuating the detected changes in linear position. If the RHP were maintained perfectly, the model would maintain gaze on a space-fixed target under conditions of linear acceleration without requiring corrective saccades to target. For an illustration, see *Heave Y - Perfect* (Section 13.15). To simulate a normal, rather than a theoretical "perfect" subject, we set the angular response to 100% of the stimulus and the linear response to 50% of the stimulus. Thus changes in angular RHP were maintained perfectly and changes in linear RHP were underestimated by 50%.

7. Drift and Saccades

Of course, the VOR is not the sole source of eye movement while attempting to maintain gaze on a fixation point. Discrepancies between eye position and fixation point can arise due to deficiencies in the VOR or because the fixation point moves relative to the world.

In our *VOR* model, eye position moves towards the fixation point at nominal fixed rates of 1°/sec in darkness and 10°/sec in light. If this slow drift is insufficient to maintain gaze on the fixation point, a saccade or quick phase is triggered.

"Drift" in this context is just the tendency to keep gaze on the target by non-vestibular means. It is stronger in the light because it is mostly visual. There is a small effect even in the darkness due to something like eye muscle somatosensory feedback.

We needed to model rates of drift in the light and dark separately because nystagmus is stronger in the dark. For example, if the net vestibular signal is 5°/sec then in darkness a nystagmus with slow phase velocity of 4°/sec (5°/sec vestibular input less 1°/sec drift) will be observed. In the light nystagmus would be suppressed because 5°/sec (vestibular input) is less than 10°/sec (drift).

We also need this mechanism to prevent the accumulation of errors. In real subjects resting rates change with adaptation. Without a drift to fixation point in darkness we would expect eye position to move out to extreme gaze angles in response to even tiny vestibular input.

In the *aVOR* app, the trigger for a saccade was simply the magnitude of the momentary angular distance from eye position to fixation point. If that distance

exceeded 10° at any moment, a saccade was generated to bring the gaze back to the fixation point.

This algorithm was considered inadequate for the present model, mainly because it permitted a persistent discrepancy of up to 10°, which the constant drift (in *aVOR*, of 20°/sec) might take many seconds to correct if VOR was deficient or the target was moving. Such a discrepancy, persisting over several seconds, is not realistic. In order to produce more natural nystagmus with saccades at a rate that increases with angular velocity of the head, the present model instead maintains an integration of angular distance moved by the head, as detected by the canals.

The integration builds at a steady base rate of 250°/sec, plus actual head angular distance moved. When this integration exceeds a value of 50° a saccade is triggered if the present discrepancy between eye position and fixation point is greater than 1°.

The effect of this algorithm is that saccadic corrections occur at least every 200ms, if required, and at shorter intervals during periods of relatively high (detected) head rotation.

8. Semicircular Canal Activation

When a semicircular canal is subject to angular acceleration, the bony and membranous canal ducts move with the head but the endolymph filling the interior of the duct tends to remain stationary due to inertia. This exerts sideways pressure on the crista ampullaris, bending the sensory hair cells and generating action potentials to flow along the vestibular afferents to the vestibular nuclei. The magnitude of the deflection of the crista depends on the magnitude of the angular acceleration in the plane of the canal. In *VOR*, each canal has an associated unit-length vector that lies approximately orthogonal to the plane of the idealised canal, see below.

Left anterior	$(-1/\sqrt{2}, 1/\sqrt{2}, 0)$
Left lateral	$(0, 0, 1)$
Left posterior	$(-1/\sqrt{2}, -1/\sqrt{2}, 0)$
Right anterior	$(1/\sqrt{2}, 1/\sqrt{2}, 0)$
Right lateral	$(0, 0, -1)$
Right posterior	$(1/\sqrt{2}, -1/\sqrt{2}, 0)$

These vectors are simplified in that the lateral canal vectors are perfectly vertical (aligned with the z axis), and the anterior and posterior canal vectors are perfectly horizontal (orthogonal to the z axis) and lie at 45 degrees to both the x and y axes. The signs of the vectors are such that positive rotation about each vector (according to the right hand rule) tends to maximally activate the sensory cells in that canal. The effective stimulus due to angular acceleration for each canal is therefore proportional to the dot product of the angular acceleration of the head and the axis vector of the canal.

The effective angular acceleration at each canal is applied to a leaky integrator to produce an estimate of angular velocity. The leaky integrator is an approximation of the physical properties of the ampullary cupula according to which angular acceleration of a canal causes pressure changes in the endolymph and thus deflection of the cupula. This deflection of the cupulae is interpreted neurally as velocity, and as the cupula returns to its resting position the interpretation of velocity returns to zero. This mechanism provides relatively accurate angular velocity signals during brief head movements, but the signal tends to decay to resting rate during long periods of constant head velocity. The simplified velocity integrator implemented in *VOR* leaks at a rate of 5% per second.

This angular velocity estimate is converted to a change in afferent firing rate (nominally 2 spikes per degree per second), multiplied by the *gain* for the canal (normally 1.0, but may be modulated by abnormal conditions), added to the resting rate (nominally 100 spikes per second), and clamped to a non-negative value (Ewald's Second Law) to produce a *simple firing rate*.

In order to simulate adaptation, the simple firing rate is passed through a finite impulse response (FIR) filter, specifically a moving average of the previous 12.5 seconds, to produce a *filtered firing rate*.

Meanwhile the vestibular nuclei maintain an *expected firing rate* for each canal. The expected firing rate drifts towards the filtered firing rate linearly at 2 Hz per second. The expected firing rate is subtracted from the filtered firing rate to produce a *result firing rate*.

Where

h = head angular acceleration

l = velocity integrator leak rate (0.05/second)

a = canal axis vector

v = velocity integrator

s = simple firing rate

g_f = canal firing rate gain (normally 1.0)

g_r = canal resting rate factor (normally 1.0)

r = resting rate

p = firing rate per degree per second

f = filtered firing rate

d = expected firing rate drift factor (2 Hz)

e = expected firing rate

r = resting rate

x = result firing rate

$v \leftarrow (1 - l)(v + h.a)$

$s = r\, g_r + v\, p\, g_f$ (s >= 0)

f = FIR(s)

if f > e + d

    e ← e + d

if f < e - d

    e ← e - d

if e - d < f < e + d

    e ← f

x = f - e

9. Canal Contributions to the *VOR* Model

In simple terms, the VOR in each of 3 axes (LAT, LARP, RALP) is driven by the difference between the activations (result firing rates) of each pair of contralateral canals:

LAT: left lateral - right lateral

LARP: left anterior - right posterior

RALP: right anterior - left posterior

In practice, the firing rate of each canal has a lower bound associated with the resting rate which cannot be inhibited below 0 spikes per second. When the firing rate at both sides does not fall below this lower bound (roughly speaking, when the head angular velocity is below about 50°/sec) the VOR is determined simply by the difference between the contralateral contributions.

At angular velocities above about 50°/sec the contribution from the negative side asymptotes to zero, and the VOR is increasingly (proportionally) driven by the contribution from the positive side. VOR gain remains around 1. Therefore there is a mechanism operating in the vestibular nuclei that progressively weights the contribution from the positive side canal when determining the change in eye direction.

Where

d = difference in firing rates from contralateral canals

r = resting rate

p = firing rate per degree per second

e = change in eye direction (degrees)

if $-r < d < r$

$e = -d / 2p$

if $d < -r$

$e = -d (1/p + r/pd)$

if $d > r$

$e = -d (1/p - r/pd)$

10.Otolith Activation

Whereas each semicircular canal is sensitive to angular acceleration around a single axis, the otolith organs are sensitive to linear acceleration across a reasonably flat plane. (To be precise, the utricular macula is curved such that the anterior is tilted upwards, but for simplicity the present model considers each macula to be planar.) The surfaces of each macula are covered with sensory hair cells. Bunches of hair cells protrude into a gelatinous layer containing otoconia, which are denser than the surrounding fluid and therefore lag linear head movements due to inertia. The hair cells are orientated on the surface of the maculae such that each cell responds maximally to acceleration in a specific direction. Each otolith organ has a curved *striola* that lies down the centre of the organ roughly longitudinally. Otolith hair cells tend to be optimally sensitive to linear acceleration along a vector that lies in the plane of the macula and generally towards the striola in the utricular macula and away from the striola in the saccular macula. The anatomy of these hair cells is such that any linear acceleration in the plane of a macula will optimally excite some of the hair cells and not others, producing a unique pattern of responses.

In the present model, each macula has an associated normal unit vector which is the mean of the unit normals at each point on its surface. The normal vectors are approximately orthogonal to the surface of the maculae:

Left utricular	(-0.79, 0.09, 0.61)
Left saccular	(0.33, -0.90, -0.29)
Right utricular	(-0.79, -0.09, 0.61)
Right saccular	(0.33, 0.90, -0.29)

Macular response to stimulus by linear acceleration is constrained to the plane orthogonal to the respective normal vector by twice calculating the cross vector product of the stimulus with the normal. The magnitude of the shear response is proportional to the sine of the angle between the acceleration stimulus and the normal vector, and is maximal when the acceleration vector lies in the macular plane.

Where

a = stimulus linear acceleration vector

n = normal to the macular plane

and r = shear response vector lying in the macular plane

$$r = n \times (a \times n)$$

VOR can display the macula normal vectors (in green) and the shear response vectors (in yellow) illustrating that the shear response vectors are always orthogonal to the normal vectors, ie. lie in the macular plane.

11.Otolith Contributions to the *VOR* Model

Linear acceleration of the head stimulates the otolith organs. In the present model, acceleration signals from the organs are integrated to produce linear velocities, which in turn adjust the position estimate for the RHP.

Head velocity along the naso-occipital axis results in convergence of the eyes. Head velocity along the vertical axis results in vertical eye movement. Head velocity along the interaural axis results in horizontal eye movement. In addition, head acceleration along the vertical axis also drives cyclovergent torsion. Finally, tilt with respect to gravity drives torsional counterroll at a nominal gain of 10%.

Consider that the acceleration information from the otolith organs is restricted to vectors that are co-planar with the maculae, and that the vectors normal to the maculae are not orthogonal. It is not possible to deduce the net acceleration applied to the otoliths simply by summing the activation vectors. For example, acceleration along the naso-occipital axis strongly stimulates both the utricle and the saccule, whereas acceleration along the vertical axis tends to stimulate the saccule more than the utricle, and acceleration along the interaural axis tends to stimulate the utricle more than the saccule. Simply adding the activation vectors would overstate acceleration along the naso-occipital axis and understate acceleration along the interaural and vertical axes.

To derive an accurate interpretation of acceleration from the otolith activation vectors, they are transformed by the inverse of the matrix which represents the sum of the saccular and utricular normal vector crosses.

Where

s = saccule normal vector

u = utricle normal vector

a = acceleration

$$m = s \times (a \times s) + u \times (a \times u)$$

$$= \begin{pmatrix} s_z^2+s_y^2+u_z^2+u_y^2 & -s_xs_y-u_xu_y & -s_xs_z-u_xu_z \\ -s_xs_y-u_xu_y & s_x^2+s_z^2+u_x^2+u_z^2 & -s_ys_z-u_yu_z \\ -s_xs_z-u_xu_z & -s_ys_z-u_yu_z & s_x^2+s_y^2+u_x^2+u_y^2 \end{pmatrix}$$

t = saccule activation vector

v = utricle activation vector

$a = (t + v)\, m^{-1}$

Although the otolith organs, like the canals, maintain a resting rate of afferent activation, this does not translate into a net activation vector in any particular direction. However there is a symmetrical imbalance between the interaural axis components of the activation vectors such that the otolith organs on each side of the head report a steady acceleration towards the centre of the head. In the present model components of this acceleration are reported by both the saccular and utricular maculae and have a magnitude of 0.5g. This resting acceleration has no effect on the resultant VOR unless acute dysfunction interrupts one signal, in which case lateral nystagmus with slow phase directed towards the affected side may be observed.

12. Application Interface

The *VOR* application was programmed in Objective-C using the Xcode integrated development environment and runs on the Apple iPad. It is controlled using settings on 3 screens: *Main Screen*, *Condition Screen* and *Motion Profile Screen*.

12.1. Main Screen

A Main Screen displays a menu bar, a 3D representation of the subject's head and optionally a time-series data chart (see Figure 2).

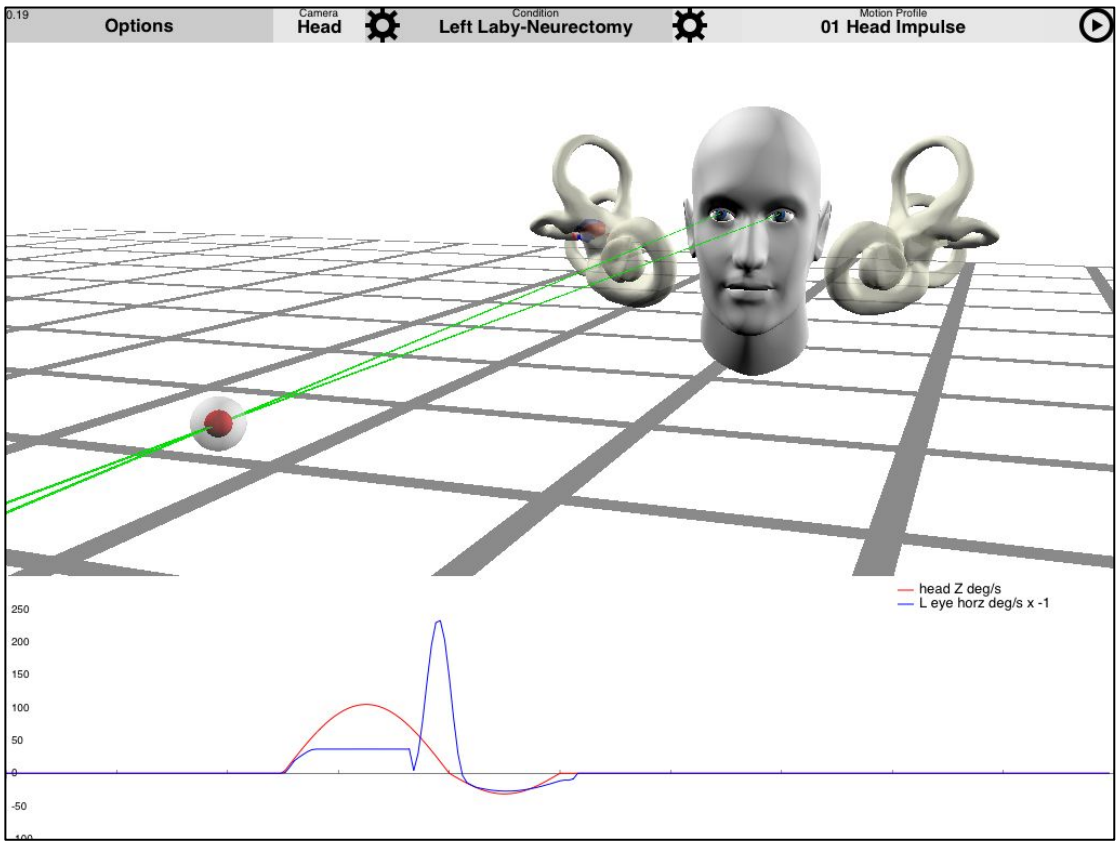

Figure 2. *VOR* Main Screen

On the Main Screen an *Options* menu selects which parts of the model are displayed in the 3D view (ground, fixation point, lines of sight, GIA vectors etc.) and allows

recording of video and data. A *Camera* menu selects whether the 3D view should be fixed relative to the world, chair or head. A *Condition* menu selects from a series of pre-set or tailored conditions for the subject, such as normal, unilateral vestibular loss (UVL), bilateral vestibular loss (BVL) etc., plus additional conditions set by the researcher, and provides entry to the Condition Screen (Section 12.2). A *Motion Profile* menu selects from a series of pre-set or tailored motion profiles to apply to the subject (head impulse, sinusoidal rotation etc. plus additional profiles set by the researcher) and provides entry to the Motion Profile screen (Section 12.3).

Figure 3 shows the Main Screen with all the options and menus revealed.

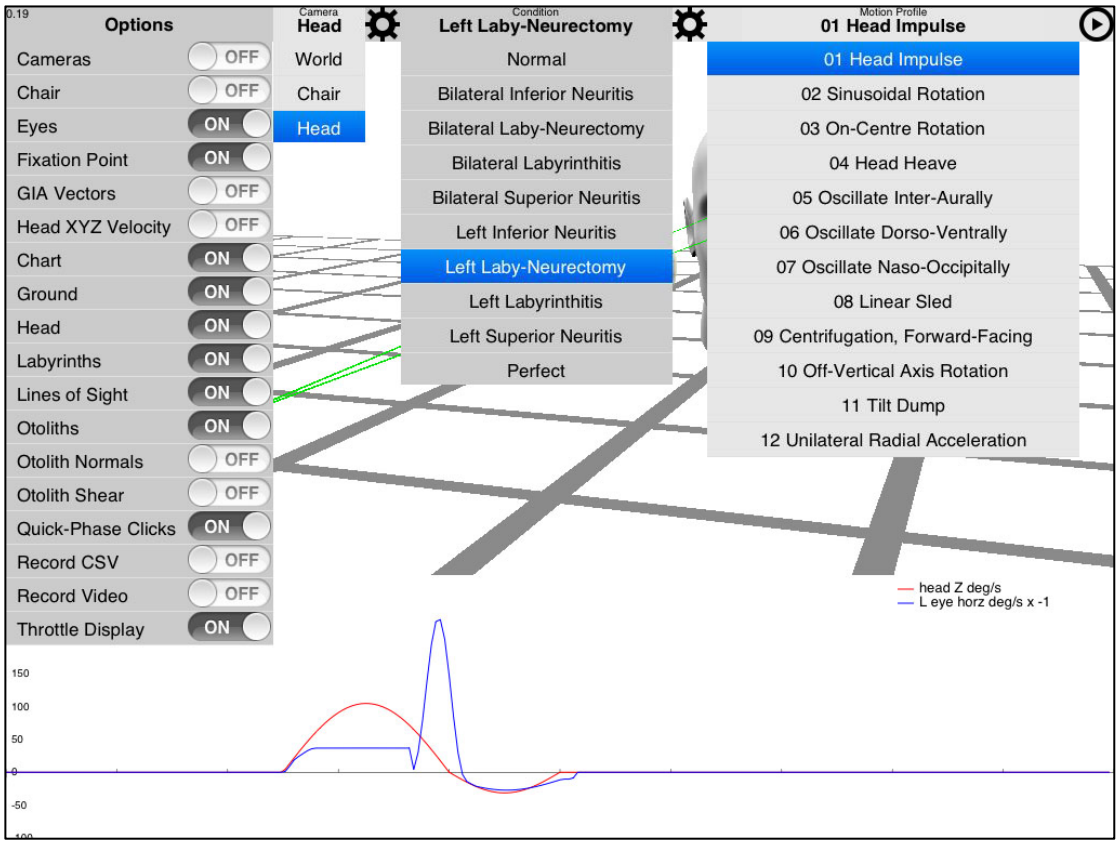

Figure 3. *VOR* Main Screen with options and menus revealed

The *Options* menu includes *Record CSV* and *Record Video* switches. If these are set, the researcher is offered the opportunity at the end of each profile run to save a

comma-separated values (CSV) format data file containing the time-series data used to draw the chart, and a screen-captured video of the profile. The data values to be charted and recorded are selected when programming the motion profile (Section 12.3). Saving the data at the end of a motion profile run creates a ZIP file accessible in the iTunes File Sharing area. The ZIP file contains:

- PDF files describing the selected condition and motion profile;
- PLIST files which can be loaded into a different *VOR* iPad to run the profile or condition;
- CSV file containing the data displayed in the chart, if requested;
- MOV file containing a screen recording of the 3D view and chart during the motion profile, if requested;
- PNG file containing the chart, if requested.

12.2. Condition Screen

The Condition Screen (see Figure 4) allows entry of:

- condition title;
- notes;
- series of gain factors to be applied to each end organ's firing and resting rates;
- drift rate in light and darkness in degrees per second;
- canal and otolith adaptation leak factors;

- quick-phase trigger values and latency (see *Drift and Saccades*, Section 7).

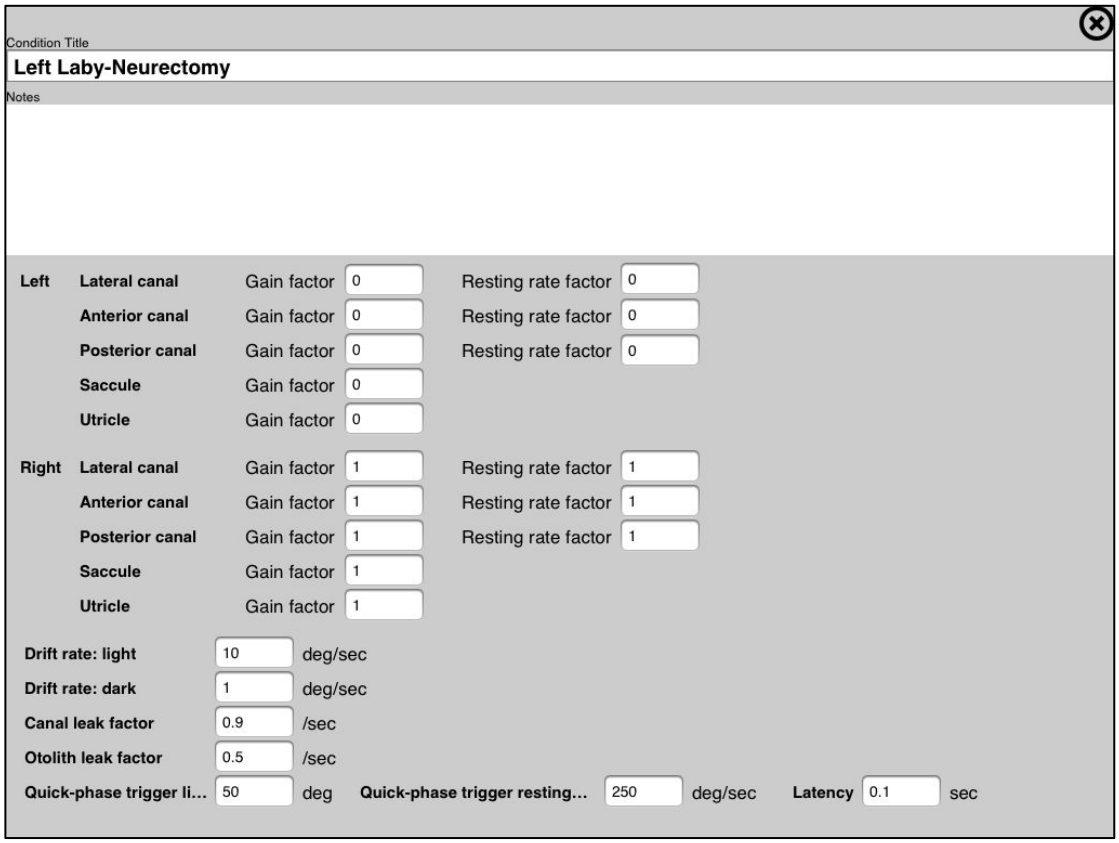

Figure 4. *VOR* Condition Screen

12.3. Motion Profile Screen

The Motion Profile Screen (see Figure 5) allows the researcher to program any series of linear and angular motions into a single profile. A profile includes:

- title;
- notes;
- whether the lights are on or off during the profile;
- whether the fixation point is fixed relative to the world, chair or head;

- whether the 3D graphic camera view is fixed relative to the world, chair or head;
- sample rate at which to calculate intermediate positions and values, chart and optionally record data;
- total duration of the profile;
- initial chair, head and fixation positions;
- initial chair and head orientations;
- minimum and maximum chart y axis labels;
- series of motion profile actions;
- list of values to be included on a chart, if required.

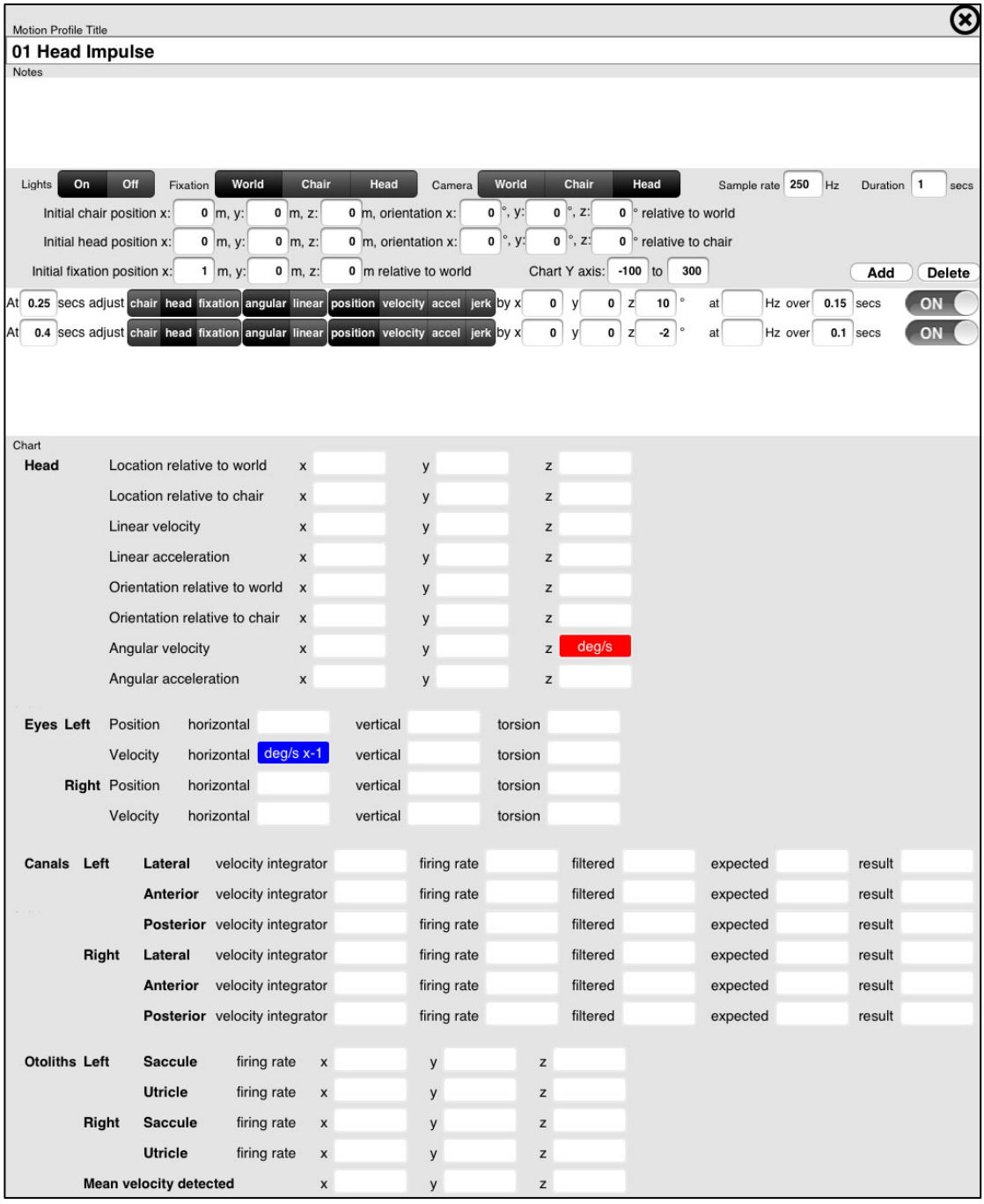

Figure 5. *VOR* Motion Profile Screen

The motion profile consists of a series of profile *actions*. An action is defined by the following settings:

- start time, relative to the start of the profile, in seconds;
- whether the action is to affect the chair, head or fixation point;

- whether the action is to affect the orientation (angular) or translation (linear) of the frame (chair, head or fixation point);

- whether the action is to change the frame's (angular or linear) position, velocity, acceleration or jerk;

- degrees (if angular) or metres (if linear) by which to change the frame's orientation or position;

- frequency at which to effect the action, if a sinusoidal (cyclic) profile action is required;

- duration of the action, in seconds.

Each action may be temporarily disabled if required.

During the motion profile, any combination of the following data values may be charted and recorded:

- head location or orientation relative to world (x, y or z component);

- head location or orientation relative to chair (x, y or z component);

- head linear or angular velocity or acceleration velocity (x, y or z component);

- left or right eye position or velocity (horizontal, vertical or torsional);

- left or right lateral, anterior or posterior canal velocity integrator, filtered firing rate, expected firing rate or result firing rate (see explanation of the canal firing rate calculation in *On-Centre Rotation*, Section 13.11);

- left or right saccule or utricle firing rate along the shear vector (x, y or z component) (see explanation of otolith shear firing vectors in *Otolith Contributions to the VOR Model*, Section 11);

- mean velocity reported by the otoliths (x, y or z component).

Linear values are in metres, metres per second etc.; angular values are in degrees, degrees per second etc. Each selected data value may be assigned a colour and scale for the chart trace and data recording.

13.Results

The following pre-set motion profiles and end organ conditions were programmed into *VOR* and various measures of interest, such as head and eye velocities, were charted and recorded in comma-separated format data files. Simultaneously video was recorded displaying the head and eye movements during each motion profile. See the Appendix for this recorded data.

13.1. Lateral Head Impulse – Normal

The Head Impulse Test (HIT) is a common test for vestibular dysfunction (eg. Halmagyi & Curthoys, 1988). It consists of a brief, unpredictable, high acceleration passive turn of around 10° to 15° around the vertical axis (close to the Lateral canal plane) while the subject fixates on a world-referenced point approximately 1 metre in front of the subject. A normal subject is expected to compensate for the turn with a smooth VOR moving the eyes by an equal angle in the opposite direction, thereby maintaining gaze on target without the need for corrective saccades. (See *01 Impulse LAT - 01 Normal - 20140909.1526* in the Appendix.) In this case we recorded the head angular velocity around the vertical axis and the compensatory left eye horizontal velocity, both in degrees per second. Eye velocity was multiplied by -1 so that it appeared on the chart in the same direction as the head velocity for the convenience of comparison. See Figure 6 for the head and left eye velocities recorded.

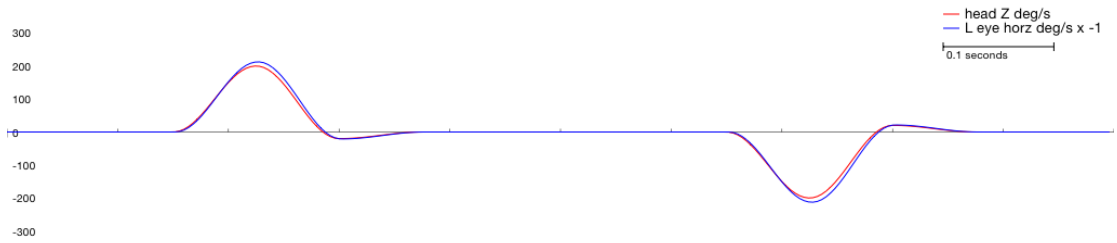

Figure 6. Head and eye velocity traces during successive contralateral head impulses around the Lateral axis in a normal subject

The *VOR* model produced an eye movement response that maintained gaze on target without corrective saccades. Notably, absolute eye velocity was slightly higher than head velocity, indicating a VOR gain slightly greater than 1, which was necessary to compensate for the lateral displacement of the eyes during the turn in addition to the angular rotation.

13.2. Lateral Head Impulse with Close Fixation – Normal

During a lateral head impulse with close world-referenced fixation point, at just 0.2m in front, a normal subject is expected to respond with a smooth VOR which is modulated by fixation distance and by the forward and lateral displacement of the eyes (resulting from their offset from the centre of head rotation) (Viirre, Tweed, Milner, & Vilis, 1986). The lateral displacement is different for each eye. During the impulse both eyes move to the left, but one moves forward (towards the target) and one moves back (away from the target). Therefore each eye needs to rotate through a different angle to remain on target. (See *02 Impulse LAT close - 01 Normal - 20140909.1529* in the Appendix.) See Figure 7 for the head and left and right eye velocities recorded.

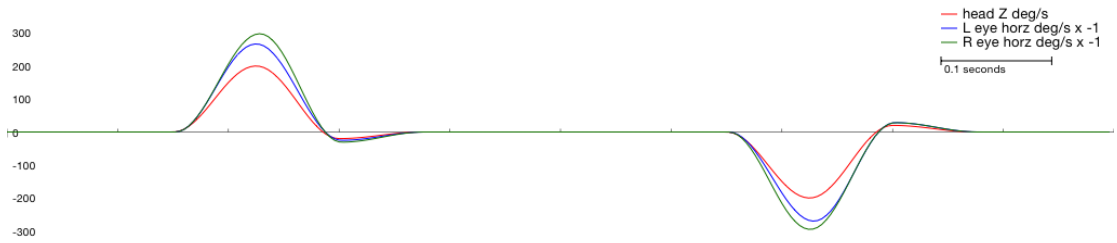

Figure 7. Head and left and right eye velocity traces during successive contralateral head impulses around the Lateral axis in a normal subject with close fixation point

The *VOR* model produced eye movement responses that maintained gaze on target without corrective saccades. Notably, both left and right eye velocities were significantly larger than head velocity to compensate for the lateral displacement of the eyes during the head impulse, and were different from each other, reflecting the different displacements of the target relative to the eye.

13.3. Lateral Head Impulse – Left Unilateral Vestibular Loss

A subject with absent function in one horizontal canal is expected to be unable to produce a smooth compensatory VOR in response to a head impulse, resulting in a corrective saccade to maintain gaze on the fixation point (Halmagyi et al., 1991). In this case we recorded the *VOR* model predictions for eye movement during a head impulse for a subject with left unilateral vestibular loss (See *01 Impulse LAT - 02 UVL Left - 20140909.1530* in the Appendix.) See Figure 8 for the head and left eye velocities recorded.

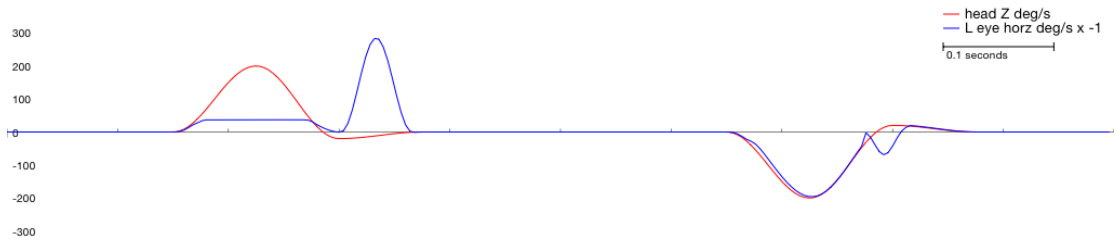

Figure 8. Head and left eye velocity traces during successive contralateral head impulses around the Lateral axis in a subject with left unilateral vestibular loss

The *VOR* model produced an eye movement with low velocity during the head impulse towards the affected side. Around 200ms after the start of the impulse the model produced a corrective saccade towards the affected side to compensate for the low VOR velocity. Some eye velocity response occurs during the impulse towards the affected side resulting from the contribution from the horizontal canal on the healthy side. Inhibition of the tonic resting rate in the healthy canal reduced the afferent signal to zero which limited the magnitude of this contribution to produce a peak eye velocity of around 40°/sec, far less than the peak head velocity of 200°/sec. The progressively increasing error in eye position relative to fixation point triggered a corrective saccade with peak velocity around 280°/sec to redirect gaze to the fixation point.

During the impulse towards the healthy side (see Figure 8), the *VOR* model produced an eye velocity response that was fairly close to head velocity, because the healthy (excited) canal produces most of the VOR response at high velocities in this direction. At these higher velocities there is less contribution from the unhealthy canal. Towards the end of the head impulse in the healthy direction the relatively small reduction in eye velocity (from the missing but minor contribution from the unhealthy

canal) triggered a small corrective saccade with peak velocity around 60°/sec (Weber, Aw, Todd, McGarvie, Pratap, et al., 2008).

13.4. Lateral Head Impulse – Bilateral Vestibular Loss

A subject with total bilateral vestibular loss is expected to be unable to produce compensatory VOR and will therefore require corrective saccades during head impulses in both directions (Weber, Aw, Todd, McGarvie, Curthoys, et al., 2008). (See *01 Impulse LAT - 03 BVL - 20140909.1530* in the Appendix.) See Figure 9 for the head and left eye velocities recorded.

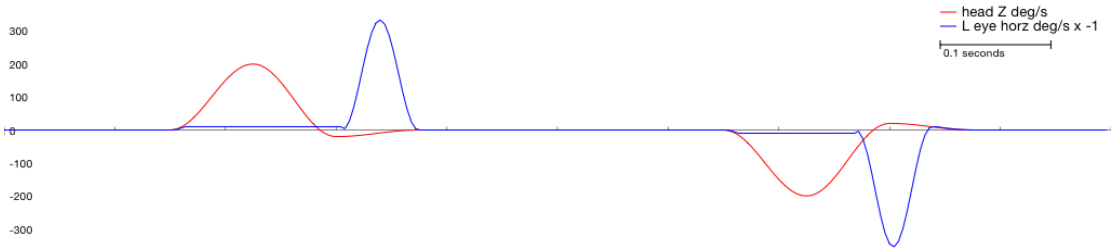

Figure 9. Head and left eye velocities during successive contralateral head impulses around the Lateral axis in a subject with total bilateral vestibular loss

The model produced a small eye velocity towards the fixation target reflecting the slow drift towards target assumed by the model at a rate of 10°/sec. However no VOR eye movement was generated. Around 200ms after the start of the head impulse in each direction a corrective saccade towards the fixation point was generated at peak velocity around 350°/sec.

13.5. Lateral Head Impulse – Left Superior Neuritis

We simulated a left superior neuritis by adjusting the gain in the left lateral and anterior canals, and left utricle, by a factor of 0.3. Thus we would expect the VOR response in a Lateral head impulse towards the affected (left) side to be significantly

impaired (MacDougall, Weber, McGarvie, Halmagyi, & Curthoys, 2009). (See *01 Impulse LAT - 04 Superior Neuritis Left - 20140909.1531* in the Appendix.) See Figure 10 for the head and left eye velocities recorded.

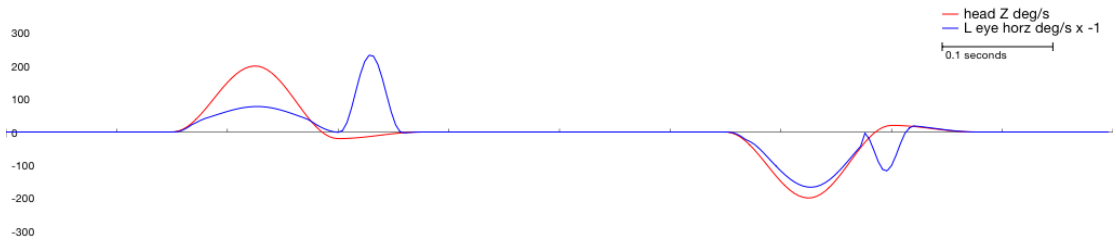

Figure 10. Head and left eye velocities during successive contralateral head impulses around the Lateral axis in a subject with left superior neuritis

The *VOR* model produced a significantly attenuated eye velocity during head impulse towards the affected side of about 35% of the head velocity, reflecting the reduced gain in the left lateral canal. This mismatch between head and eye velocity required a corrective saccade at the end of the impulse at a peak velocity around 230°/sec. The VOR away from the affected side showed less impairment and an eye velocity around 85% of head velocity, reflecting the major contribution of the lateral canal on the healthy side in the VOR response. Nevertheless the attenuated VOR response required a relatively small corrective saccade with peak velocity around 115°/sec.

13.6. LARP Head Impulse - Normal

A normal subject subjected to a head impulse of around 15° in the Left Anterior - Right Posterior (LARP) plane is expected to produce compensatory eye movements in the LARP plane (MacDougall, McGarvie, Halmagyi, Curthoys, & Weber, 2013). (See *03 Impulse LARP - 01 Normal - 20140909.1611* in the Appendix.)

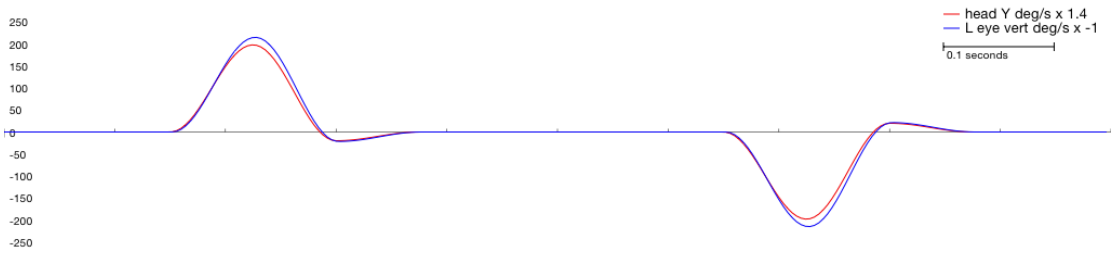

Figure 11. Head velocity around the y axis, and vertical eye velocity during successive contralateral head impulses around the LARP axis in a normal subject

Figure 11 records the velocity around the world y axis with the head offset by 45° yaw, multiplied by a factor of 1.4 to represent the velocity in the LARP plane, and the vertical eye velocity. Gain is slightly greater than 1, compensating for the lateral displacement of the eyes during the impulse in addition to the angular motion of the head.

13.7. LARP Head Impulse - Left Superior Neuritis

A subject with a left superior neuritis is expected to be unable to produce accurate compensatory VOR during head impulses in the LARP plane and will display corrective saccades to maintain fixation on the world-referenced target (MacDougall et al., 2013). (See *03 Impulse LARP - 04 Superior Neuritis Left - 20140909.1531* in the Appendix.) The traces of head and eye velocity are similar to those recorded during a head impulse in the Lateral plane in a subject with a left superior neuritis.

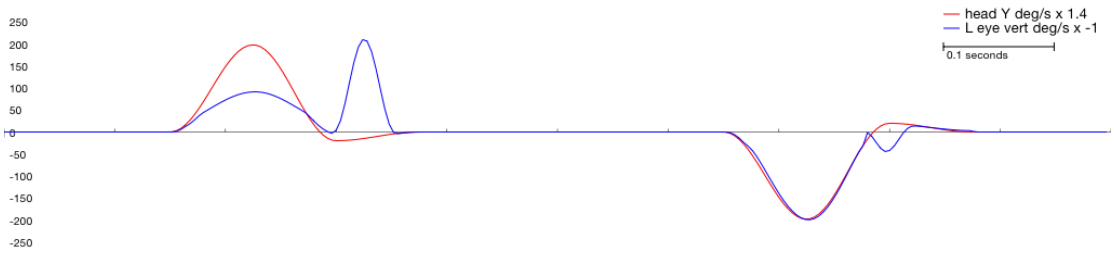

Figure 12. Head and left eye velocities during successive contralateral head impulses around the LARP axis in a subject with left superior neuritis

Figure 12 includes the left eye velocity predicted by the *VOR* model. Eye velocity during the impulse towards the affected side is around 35% of head velocity, and a corrective saccade is generated to regain fixation on the target. Eye velocity during the impulse away from the affected side is nearly sufficient to maintain fixation, requiring only a small corrective saccade to regain fixation.

This saccade asymmetry can assist a clinician in diagnosis of specific canal dysfunction.

13.8. Sinusoidal Yaw - Normal

VOR was programmed to rotate the chair sinusoidally around the vertical axis with an amplitude of 30° and frequency 0.5Hz. A normal subject would be expected to maintain gaze on a world-reference fixation point without requiring corrective saccades (Wolfe, Engelken, & Kos, 1977). (See *05 Sinusoidal Yaw - 01 Normal - 20140909.1532* in the Appendix.)

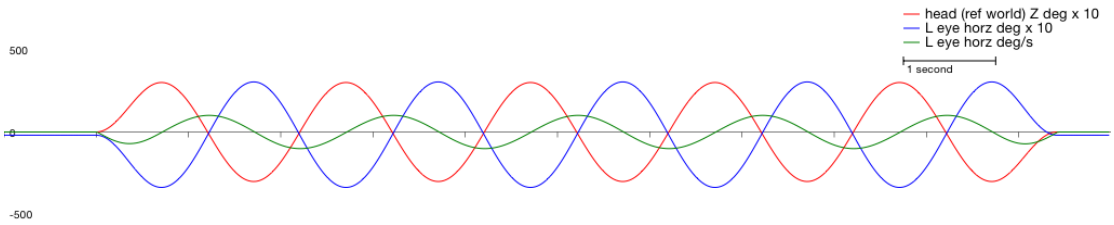

Figure 13. Head orientation and left eye horizontal position and velocity during sinusoidal yaw in a normal subject

The red trace in Figure 13 describes the vertical axis orientation of the head and the blue trace describes the left eye horizontal position. The *VOR* model predicted compensatory VOR maintaining gaze on a world-referenced fixation point with eye position mirroring head position.

13.9. Sinusoidal Yaw - Unilateral Vestibular Loss

A subject with complete unilateral vestibular loss is expected to be unable to maintain gaze on a world-referenced fixation point during sinusoidal rotation around the vertical axis, requiring periodic corrective saccades (Baloh, Honrubia, Yee, & Hess, 1984; Paige, 1983). At sufficiently high velocities these saccades are expected to be of greater amplitude and velocity when the head is turning towards the affected side, because the canal that makes a larger contribution in this direction is unhealthy. During the sinusoidal phase when the head is turning away from the affected side the VOR is impaired to a lesser extent because the healthy canal makes a larger contribution in this direction. (See *05 Sinusoidal Yaw - 02 UVL Left - 20140909.1532* in the Appendix.)

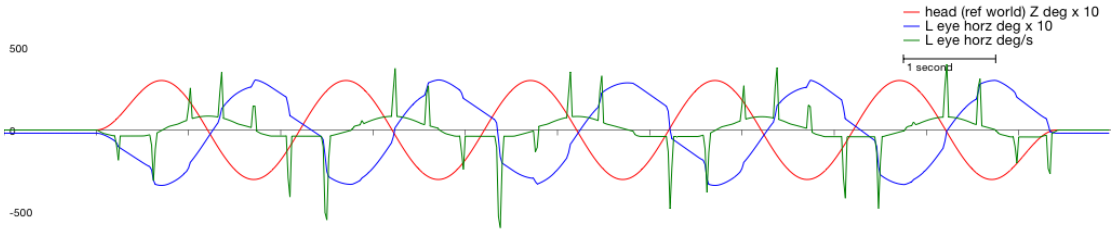

Figure 14. Head yaw and horizontal eye position and velocity during sinusoidal yaw in a subject with complete unilateral vestibular loss

As shown in Figure 14, the *VOR* model predicts two or three corrective saccades during each directional phase of the sinusoidal cycle. Saccades during rotation toward the affected side have amplitude of up to around 25° and velocities up to 500°/sec, whereas saccades during rotation away from the affected side are smaller, with amplitudes of around 10° and velocities of around 300°/sec.

13.10. Sinusoidal Yaw - Bilateral Vestibular Loss

During sinusoidal rotation around the vertical axis, a subject with complete bilateral vestibular loss is expected to be unable to maintain gaze on a world-referenced fixation point without large corrective saccades during rotations in both directional phases of the cycle (Honrubia et al., 1985). (See *05 Sinusoidal Yaw - 03 BVL - 20140909.1532* in the Appendix.)

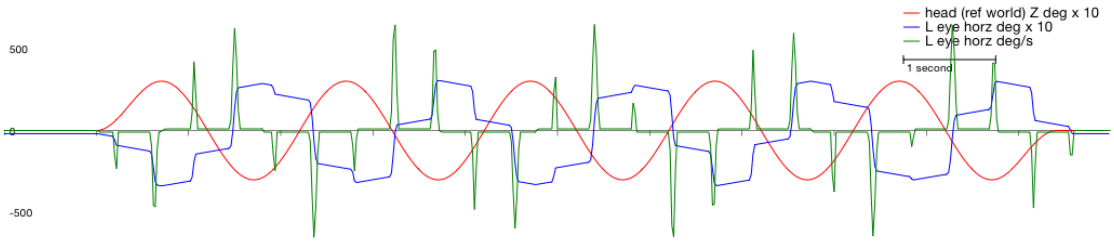

Figure 15. Head yaw and horizontal eye position and velocity during sinusoidal yaw in a subject with complete bilateral vestibular loss

As shown in Figure 15, the *VOR* model predicts no smooth VOR responses and one or two large corrective saccades in each direction of rotation with amplitude around 35° and velocity up to around 600°/sec.

13.11. On-Centre Rotation

During on-centre rotation, the subject's head is positioned upright and centred around the vertical axis of the rotating chair, with a chair-fixed fixation point 1m in front of the subject. The chair is then accelerated around the vertical axis for example to 200°/sec over 20 seconds (acceleration 10°/sec^2), maintained at 200°/sec for 60 seconds, then decelerated to stationary over 20 seconds (see *06 On-Centre Rotation - velocities - 01 Normal - 20140909.1536* and *06 On-Centre Rotation - firing rates - 01 Normal - 20140909.1533* in the Appendix).

A normal subject would be expected to be unable to maintain gaze on the fixation point during acceleration because the VOR tends to direct the eyes in the direction opposite to the rotation of the head. The subject generates successive corrective saccades to refixate on the target, which appear as nystagmus. The quick phases of the nystagmus are in the direction of rotation. The amplitude of the saccades increases during acceleration to maximum head angular velocity, and thereafter progressively decreases as the vestibular system is unable to transduce constant velocity rotation until the nystagmus disappears entirely. At this point the subject is able to fixate steadily on the head-referenced target.

A few seconds after the nystagmus ceases, a few "beats" of secondary nystagmus appear as a result of adaptation to the prolonged acceleration. During secondary nystagmus the direction of the quick phases is opposite to the direction of head rotation. Secondary nystagmus lasts a few seconds, and thereafter the subject is able

to maintain gaze on the fixation point while the chair maintains a constant rate of rotation.

As the subject attempts to maintain gaze on the fixation point while the chair decelerates from 200°/sec to stationary, nystagmus appears again, but during this period the quick phases are contra-rotation. The amplitude of the nystagmus increases as the chair accelerates in the opposite direction (back to rest). A few beats of secondary nystagmus may be seen after being stationary for a few seconds (Raphan, Matsuo, & Cohen, 1979). Eye velocity responses to the on-centre rotation profile according to the *VOR* model appear in Figure 16.

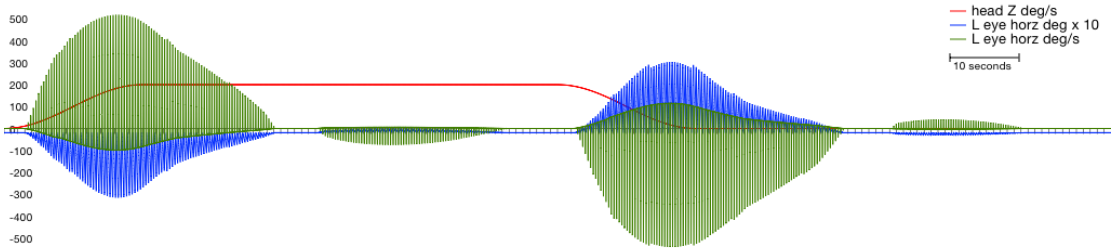

Figure 16. Head angular velocity and left eye position and velocity during on-centre rotation

Hypothesised firing rate values appear in Figure 17.

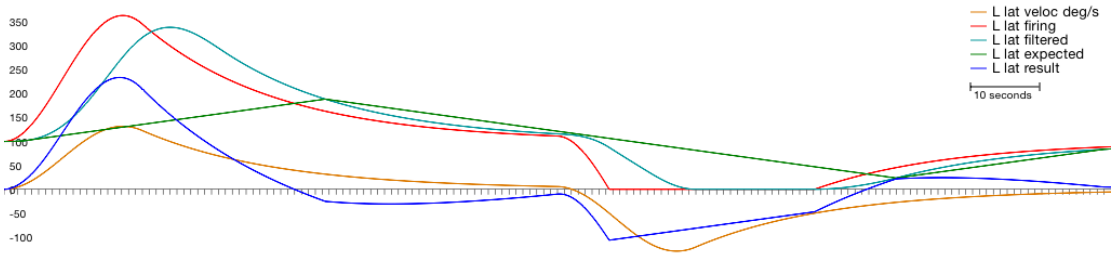

Figure 17. Left lateral canal velocity integrator and simple, filtered, expected and result firing rates during on-centre rotation

According to the *VOR* model there are multiple stages of processing between SCC motion and ocular effects:

1. The applied angular acceleration around the vertical axis, detected by the left lateral canal cupula, is applied to a notional local velocity storage integrator. The integration "leaks" velocity and in the *VOR* model the leak rate is 5% per second. Thus short duration changes in velocity may be interpreted reasonably accurately, whereas over longer periods the velocity interpretation tends to drift towards zero. This velocity is represented in Figure 17 as "L lat veloc deg/s" and increases to a maximum of around 130°/sec as the chair slowly accelerates to 200°/sec, decaying towards zero as the chair maintains constant velocity.

2. Afferent input directly from the canal is represented in Figure 17 as "L lat firing" and is modelled simply as 2 spikes per degree per sec of angular velocity (after the leaky integrator described above). Thus the firing rate increases from a resting rate of 100 spikes/sec to a maximum of around 360 spikes/sec as the velocity reaches its maximum 130°/sec, then decays back to the resting rate of 100 spikes/sec as the chair maintains constant velocity and the velocity storage integrator leaks back to zero.

   When the chair decelerates the firing rate of the left canal rapidly decreases to zero. At this point the firing rate of the contralateral canal will still be increasing and afferent input from that canal becomes the major source of vestibular drive.

3. We hypothesise that the process of adaptation can be conceptualised as the vestibular neural apparatus maintaining an "expected firing rate" (shown in Figure 17 as "L lat expected"), which drifts slowly and at a constant rate

towards the current firing rate.

The expected firing rate is calculated in two stages:

a. The afferent firing rate is passed through a Finite Impulse Response (FIR) filter which calculates a moving average firing rate over the previous 12.5 seconds (shown in Figure 17 as "L lat filtered").

b. The expected firing rate drifts towards this filtered firing rate linearly at a fixed rate of 2 spikes per second per second.

4. Finally, a "result" or effective firing rate (shown in Figure 17 as "L lat result") is calculated by subtracting the expected firing rate from the raw firing rate. The result rate drives the VOR directly.

As the result firing rate drives the VOR, the subject gaze moves away from the fixation target. The *VOR* model periodically generates a corrective saccade according to the formula described in *Drift and Saccades* (Section 7). This sequence of saccades appears as rotational nystagmus. The quick-phase amplitudes and velocities increase as the chair angular velocity accelerates. When the chair is rotating at a constant velocity, the amplitude and velocity of the quick phases decays to zero.

As described above, the resulting firing rate is dependent on an expected rate which has 2 components: a moving average filter over 12.5 seconds, and a linear drift towards this rate at 2 spikes per second. An implication of this arrangement is that as the raw firing rate decays during adaptation to the rotation and due to lag introduced by the filter, there is a period when the expected firing rate is significantly greater than the raw firing rate. In the present profile this period begins 40 seconds from the

beginning of the profile, which is 20 seconds after the initial acceleration ends. While the expected firing rate is significantly greater than the actual firing rate the VOR is directed in the opposite direction and secondary nystagmus can be observed with quick phases in the same direction as the chair rotation.

At 80 seconds into the motion profile, when the chair begins to decelerate, the velocity storage integrator has already leaked very nearly to zero. The deceleration is then interpreted as acceleration in the opposite direction. The left lateral canal is inhibited and its afferent firing rate quickly drops to zero. The contralateral canal provides the major part of the influence on the VOR.

13.12. Heave Y - Normal

During linear acceleration, the canals are not stimulated. Instead the hair cells of the utricular and saccular macula are bent by the linear inertia of a layer of otoconia. Since these hair cells are maximally excited/inhibited in a certain preferred direction and since these preferred directions are arranged at various angles in each macula, linear acceleration in various directions can be encoded and provides input to the VOR. We programmed the *VOR* model to simulate rapid linear displacements of the head along the interaural axis; first 10cm towards the subject's left (positive) over 150ms then after a delay of 500ms a similar displacement of 10cm towards the subject's right (negative) over 150ms, while fixating on a world-stationary point 1m ahead. (See *07 Heave Y - 01 Normal - 20140909.1539* in the Appendix.)

A normal subject would be expected to exhibit a linear VOR compensating to a limited extent for the head motion to help keep gaze on a world fixed target (Ramat, Zee, & Minor, 2001). It is known that the linear component of VOR acts with insufficient gain to maintain perfect gaze on a world-stationary fixation point during

rapid linear accelerations. Thus although we would expect to see a horizontal rotation of the eyes due to linear VOR, the eye movement is insufficient to maintain gaze on the fixation point, and a normal subject would produce a corrective saccade.

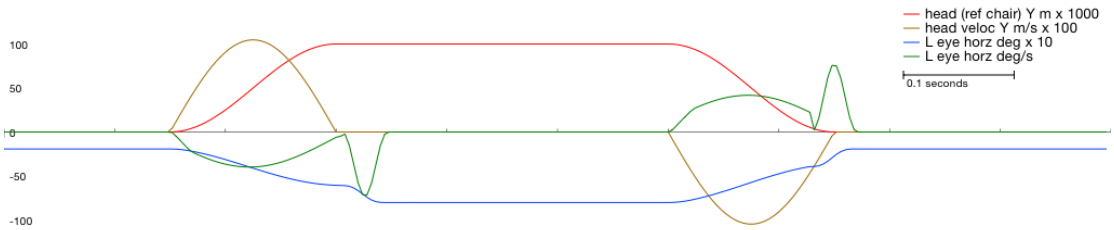

Figure 18. Head and left eye positions and velocities during brief rapid interaural motion in a normal subject

The *VOR* model predicted rapid, brief eye rotation in the opposite direction to the displacement of the head, (ie. in the direction of motion relative to the head of a world fixed target) followed by a corrective saccade around 10ms after the end of the head movement, as shown in Figure 18. Eye position and velocity shows approximately equal and opposite behaviour during the rapid linear head movement back to the starting position.

13.13. Heave Y - Left Unilateral Vestibular Loss

A subject with unilateral vestibular loss is expected to exhibit a reduced linear VOR during brief rapid displacement along the interaural axis (Crane, Tian, Wiest, & Demer, 2003). During acceleration in either direction, the utricular macula on the healthy side provides some contribution to ocular compensation but the gain is approximately half that of a normal subject. Therefore a larger amplitude corrective saccade is required to regain fixation. (See *07 Heave Y - 02 UVL Left - 20140909.1539* in the Appendix.)

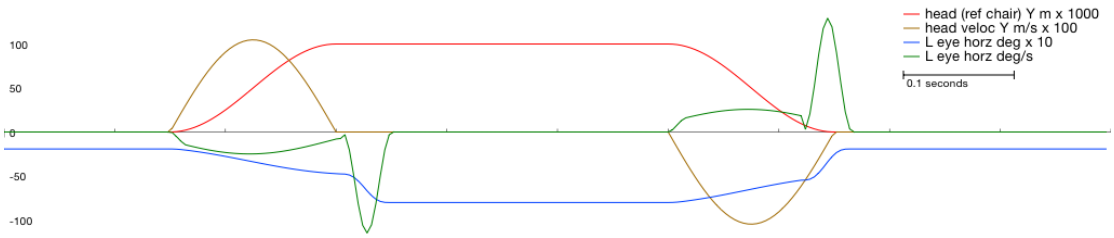

Figure 19. Head and left eye positions and velocities during brief rapid interaural motion in a subject with UVL

As seen in Figure 19, the model predicted an attenuated linear VOR response during the head displacement with a gain approximately half that of a normal subject. The corrective saccade at the end of the displacement accordingly had around double the amplitude and peak velocity.

13.14. Heave Y - Bilateral Vestibular Loss

A subject with complete bilateral vestibular loss is expected to exhibit no linear VOR whatsoever during rapid linear displacement of the head, and the only mechanism by which such a subject can maintain gaze on the world-referenced fixation point is by corrective saccades. (See *07 Heave Y - 03 BVL - 20140909.1539* in the Appendix.)

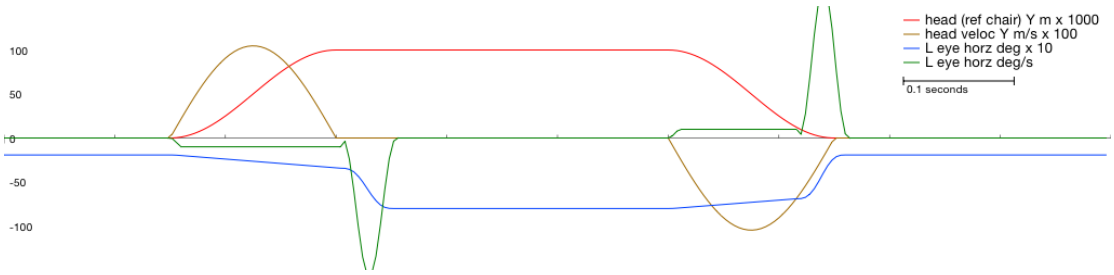

Figure 20. Head and left eye positions and velocities during brief rapid interaural motion in a subject with BVL

The *VOR* model predicted low, constant eye velocity of just 10°/sec during brief, rapid interaural head displacement, as shown in Figure 20. A slow, fixed drift to

target makes this contribution to eye position, which occurs whenever gaze on the fixation point has been lost and is generally inadequate to regain fixation during a head movement of up to 1m/sec. A corrective saccade with peak velocity around 150°/sec is generated around 150ms after the start of the displacement.

13.15. Heave Y - Perfect

Linear VOR in real subjects is imperfect, operating with a gain of around 0.5. Thus a real subject is always expected to generate corrective saccades to maintain gaze on a world-referenced fixation point during linear head displacement. The *VOR* model usually applies a gain of 0.5 to otolith activation before using the activation to drive eye position. As an illustration of the mechanism by which the *VOR* model operates, we included an example of linear VOR with gain of 1.0. (See *07 Heave Y - 05 Perfect - 20140909.1540* in the Appendix.)

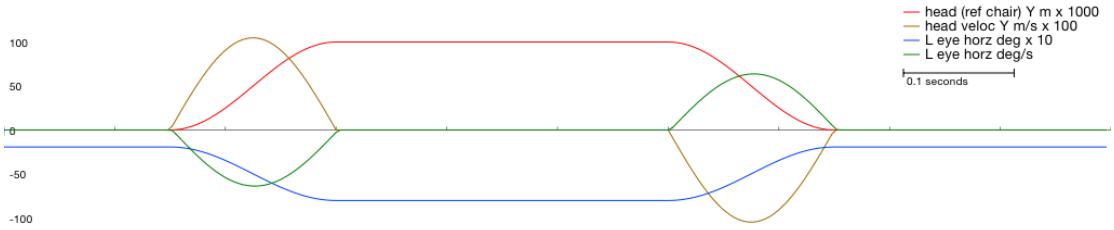

Figure 21. Head and left eye positions and velocities during brief rapid interaural displacement in a theoretical perfect subject with LVOR gain of 1.0

In a theoretical subject with perfect linear VOR, ie. with otolithic gain of 1.0, gaze is maintained on a world-referenced fixation point during rapid linear head displacement without requiring corrective saccades (see Figure 21). This illustrates the core principle of the *VOR* model - that with perfect end organ sensitivity the theoretical RHP maintains perfect gaze on a static world-referenced fixation point without requiring corrective saccades.

13.16. Oscillate Y - Normal

During oscillating linear displacement along the interaural axis with amplitude 0.3m and frequency 0.25Hz, a normal subject instructed to maintain fixation on a static world-referenced point 1m ahead is expected to exhibit some linear VOR but will be unable to maintain gaze without frequent corrective saccades (Angelaki, 2004). (See *08 Oscillate Y - 01 Normal - 20140909.1541* in the Appendix.)

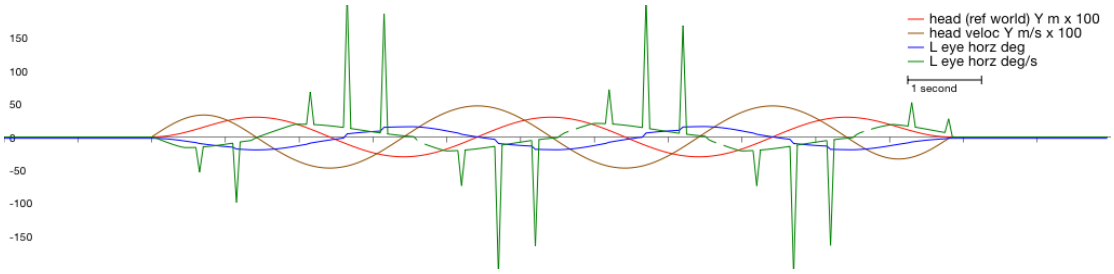

Figure 22. Head and left eye positions and velocities during interaural linear oscillation in a normal subject

At peak head linear velocity of 0.5m/s the static world-referenced fixation point 1m distant is moving horizontally across the subject's field of view at a relative angular velocity of 30°/sec. The *VOR* model predicted that in a normal subject the combination of linear VOR and drift toward target would produce peak eye velocity of only around 20°/sec and that around 3 corrective saccades in each phase would be required to maintain gaze on the fixation point, as shown in Figure 22.

13.17. Oscillate Y - Perfect

Further illustrating the principle of the *VOR* model maintaining a perfect representation of head position relative to static world-referenced fixation point to the extent of the accuracy of interpretation of end organ afferent input, the *VOR* model was programmed with an oscillating linear head displacement along the interaural

axis with amplitude 0.3m and frequency 0.25Hz and theoretically perfect VOR (see *08 Oscillate Y - 05 Perfect - 20140909.1541* in the Appendix.)

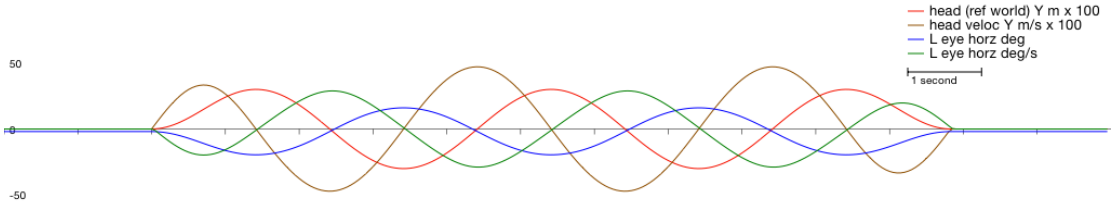

Figure 23. Head and left eye positions and velocities during linear interaural oscillation in a theoretical perfect subject with LVOR gain of 1.0

As shown in Figure 23, a theoretical subject with perfect linear VOR would be able to maintain gaze on a static world-referenced fixation point without requiring corrective saccades (Angelaki, 2004). At peak head linear velocity of 0.5m/sec the fixation point appears to move horizontally at an angular velocity of 30°/sec relative to the subject's head, and linear VOR drives eye position at an equal velocity in the opposite direction, allowing perfect maintenance of fixation.

13.18. Oscillate Z - Normal

In a normal subject during sinusoidal linear oscillation along the vertical axis, two components of eye movement can be observed. Vertical eye position responds smoothly to head vertical linear displacement but at a gain of only around one half of what would be required to maintain gaze on the fixation point (Angelaki, 2004). Corrective saccades are observed periodically as the subject works to maintain fixation. Simultaneously a small but detectable cyclovergence can be observed, with the eyes intorted during phases of higher effective gravity and extorted during phases of lower effective gravity (Olasagasti, Bockisch, Zee, & Straumann, 2008). (See *09 Oscillate Z - 01 Normal - 20140909.1542* in the Appendix.)

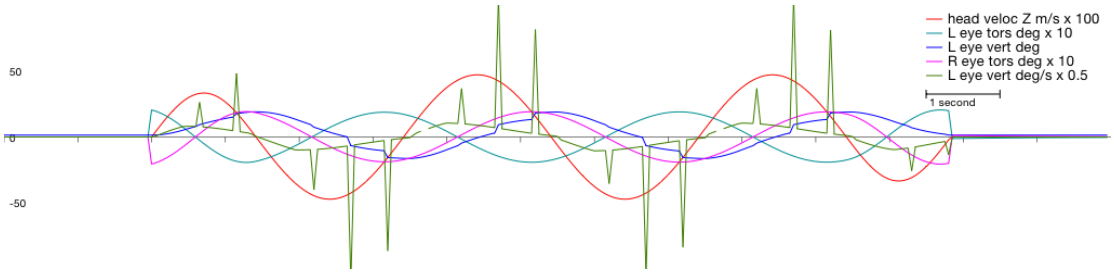

Figure 24. Head position and linear velocity, and eye vertical and torsional positions during linear vertical axis oscillation in a normal subject

As shown in Figure 24 the *VOR* model predicted left eye vertical position driven weakly by VOR to partially compensate for linear head displacement at a peak of around 20°/sec in response to angular velocity of the fixation point relative to the head of around 30°/sec, requiring periodic corrective saccades to regain fixation. Simultaneously the *VOR* model predicted cyclovergence at a peak of around 1.9° coinciding with moments of zero head velocity (maximal acceleration).

13.19. Oscillate X - Normal

A normal subject, oscillating linearly along the naso-occipital axis with amplitude 0.5m and frequency 0.5Hz would be expected to maintain gaze on a static world-referenced fixation point 1m in front of the head (at start; thereafter oscillating between 0.5m and 1.5m in front of the head) without exhibiting corrective saccades (Angelaki, 2004). (See *10 Oscillate X - 01 Normal - 20140909.1543* in the Appendix.)

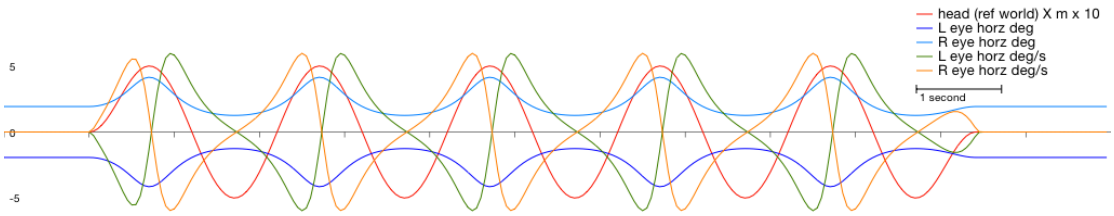

Figure 25. Head position and binocular horizontal positions and velocities during linear naso-occipital oscillation in a normal subject

The *VOR* model predicts that a normal subject can maintain fixation without required corrective saccades, despite the attenuated linear contribution to VOR. This is because the model provides for a steady drift of fixation towards target at up to 10°/sec regardless of VOR. In fact it should be noted in Figure 25 that horizontal (convergent/divergent) eye velocities are always well below this level in this motion profile and therefore all eye movements can be explained by drift.

13.20. Linear Sled Y - Normal

A subject would be expected to be unable to maintain gaze at a head-referenced fixation point during interaural linear acceleration because linear VOR tends to direct the eyes towards the world-referenced point (Niven, Hixson, & Correia, 1966). Occasional saccades would correct the gaze to the head-referenced point (see *11 Linear Sled Y - 01 Normal - 20140909.1544* in the Appendix).

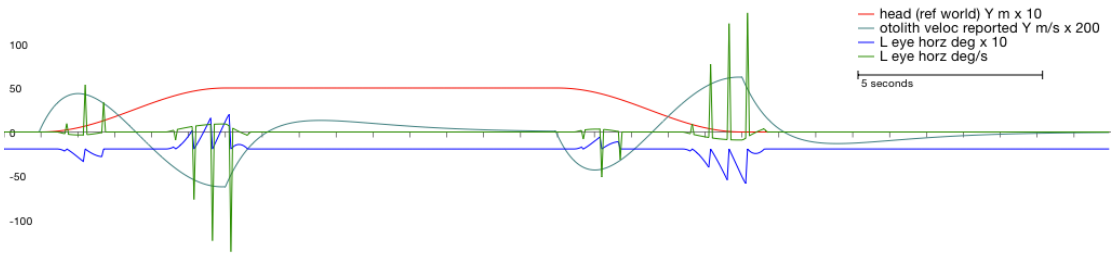

Figure 26. Head position and eye position and velocity during interaural linear acceleration in a normal subject

As shown in Figure 26, the *VOR* model predicts 2 or 3 small corrective saccades with peak velocity up to around 50°/sec during interaural linear acceleration and 3 or 4 larger saccades with peak velocity up to around 135°/sec during deceleration. The source of the asymmetry between the number and amplitude of saccades in the acceleration and deceleration phases is revealed by the trace labelled "otolith veloc reported" which shows the interaural component of the internal linear deceleration signal that is significantly damped (leading to low gain and poor sustained responses).

13.21. Centrifugation, Forward-Facing - Normal

Consider a subject on a rotating chair, 1m from the centre of rotation and facing forwards, as the chair accelerates to 200°/sec over 20 seconds, maintains constant angular velocity for 25 seconds, then decelerates to stationary over a further 20 seconds. (See *12 Centrifugation Forward - 01 Normal - 20140909.1544* in the Appendix.)

A normal subject would be expected to exhibit rotational nystagmus with quick-phases increasing in amplitude and opposite to the direction of rotation during acceleration, then decaying and eventually disappearing during the period of constant velocity. During deceleration the subject would be expected to exhibit nystagmus with quick-phases in the direction of rotation, reaching maximum amplitude as the

chair ceases rotation and continuing to decay over the following 40 seconds (Curthoys, Wearne, Dai, Halmagyi, & Holden, 1992).

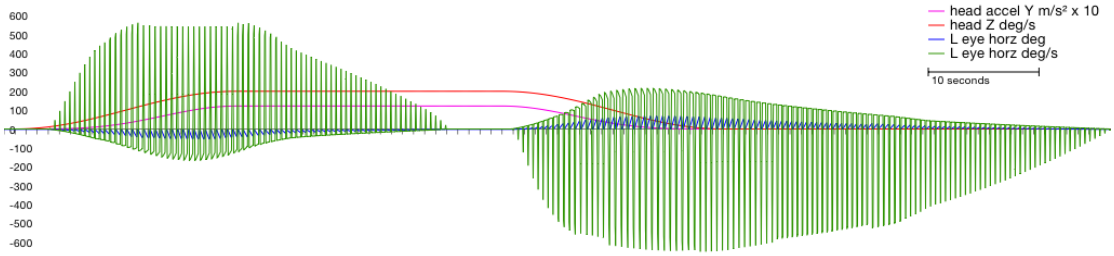

Figure 27. Head angular velocity, interaural linear acceleration and horizontal eye movement during forward-facing centrifugation in a normal subject

As the *VOR* model reveals, there are two sources of the rotational nystagmus exhibited by a normal subject during centrifugation: an angular component derived from the activation of the canals, combined with a linear component from the otoliths. As shown in Figure 27, the head linear acceleration labelled "head accel Y m/s^2 x 10" and angular velocity marked "head Z deg/s" combine additively when the subject faces forward on the rotating chair. Quick-phase peak velocity is around 500°/sec during centrifugal acceleration.

13.22. Centrifugation, Backward-Facing - Normal

A normal subject undergoing backward-facing centrifugation exhibits smaller amplitude quick-phases during the rotational nystagmus that appears during acceleration than when undergoing forward-facing centrifugation (Curthoys et al., 1992) (see *13 Centrifugation Backward - 01 Normal - 20140909.1546* in the Appendix).

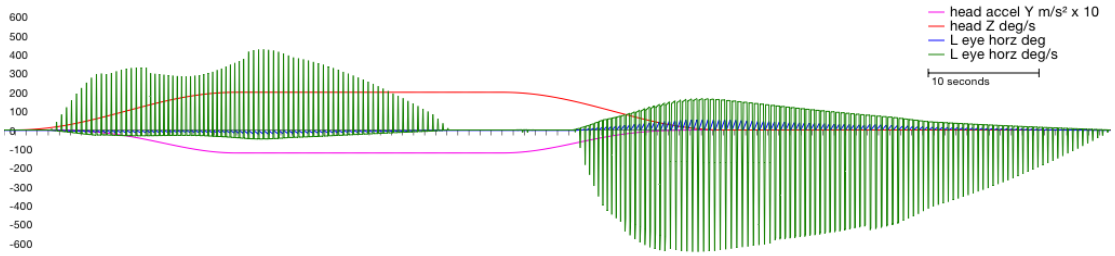

Figure 28. Head angular velocity, interaural linear acceleration and horizontal eye movement during backward-facing centrifugation in a normal subject

In contrast to forward-facing centrifugation, during backward-facing centrifugation the angular and linear components of the VOR are subtractive. As can be seen in Figure 28, head acceleration along the interaural axis counteracts head angular velocity around the vertical axis and the amplitude and velocity of quick-phases during the acceleration phase of the motion profile are attenuated to a peak of around 400°/sec.

13.23. Off-Vertical Axis Rotation - Normal

Off-vertical axis rotation (OVAR) is rotation about an axis offset by a constant angle from the vertical axis. During OVAR a subject would be expected to exhibit horizontal nystagmus with quick-phase amplitude and velocity comparable with on-vertical axis rotation at the same angular velocity. However during OVAR nystagmus decays and disappears as the VOR adapts to constant angular velocity, whereas during off-vertical axis rotation the rotational nystagmus does not decay to zero (Guedry, 1996; Harris, 1987) (see *14 OVAR - 01 Normal - 20140909.1549* in the Appendix).

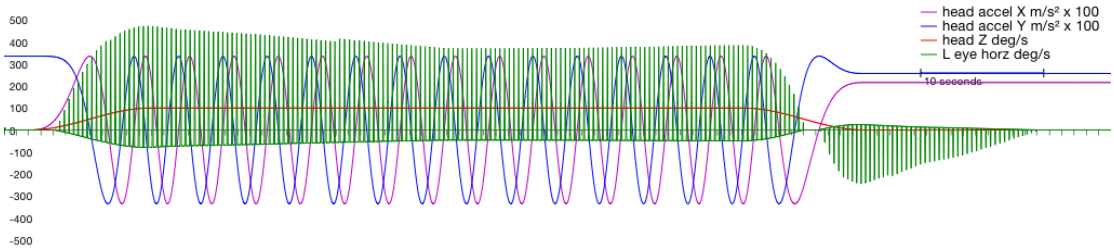

Figure 29. Head x and y components of GIA, head angular velocity and eye horizontal velocity during OVAR in a normal subject

According to the *VOR* model, the sensing of head angular velocity derives not only from canal afferents but also from the detected rotation of the GIA vector around the head. The model calculates the arctangent of the naso-occipital and interaural components of gravitational acceleration components to determine the angle of this acceleration vector, and the rate of change of this calculated angle is interpreted as angular velocity around the vertical axis. The model also calculates a "confidence level" as the cross product of the head GIA with true vertical - effectively, the greater the angle off-vertical, the greater confidence the model puts in the otolithic component of angular velocity. With the head upright and rotating around the vertical axis there is no useful rotation information to be derived so this confidence value is zero. In the "barbecue spit" configuration this confidence value tends to 100% and in this case the otolith contribution to the sensing of rotation can override that from the canals.

In the case of this example profile, rotation is at 100°/sec around an axis offset by 20° from vertical. At constant rotation the otolithic contribution to angular VOR never decays and nystagmus continues steadily with quick-phase peak eye velocity around 400°/sec (see Figure 29).

13.24. Tilt Dump - Normal

As previously discussed, a normal subject during on-centre rotation is expected to exhibit rotational nystagmus with quick-phases in the direction of rotation which decays while angular velocity is maintained. If angular velocity is then reduced to zero, nystagmus appears with quick-phases in the direction contrary to rotation, because the deceleration is interpreted by the vestibular apparatus as acceleration in the opposite direction. This nystagmus is expected to continue for a few seconds after the subject has come to rest, as the end organ afferents adapt.

However, as in the case with OVAR above, the otoliths can provide information about angular velocity if the head is off vertical. In the so-called "tilt dump" manoeuvre, the head is tilted rapidly through 30° around the naso-occipital axis shortly after the subject comes to rest, and while nystagmus caused by the angular deceleration continues. In this event the nystagmus would be expected to decay more rapidly because of the otolithic contribution to the vestibular interpretation of angular velocity (Guedry, 1992; Waespe, Cohen, & Raphan, 1985) (see *15 Tilt Dump - 01 Normal - 20140909.1551* in the Appendix).

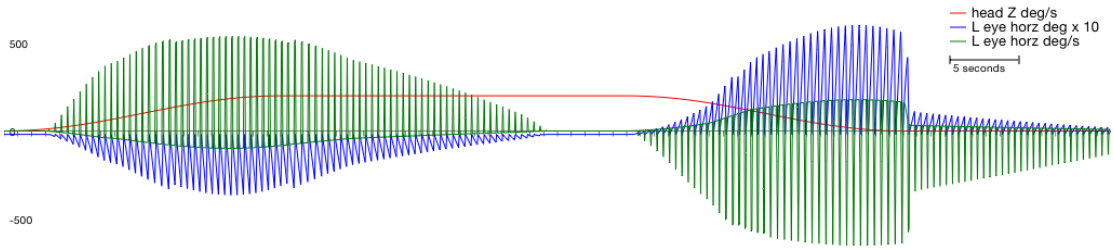

Figure 30. Head angular velocity and eye horizontal movements during tilt dump in a normal subject

Prior to the tilt of the head 5 seconds after the subject comes to a complete rest, the profile of nystagmus matches that of the simple on-centre rotation (see *On-Centre*

Rotation, Section 13.11). On tilting the head by 30° the otoliths report angular velocity of 0°/sec with "50% confidence" (sin 30° = 0.5). This immediately reduces the perceived angular velocity by 50%, as can be seen in Figure 30 where the nystagmus quick-phase velocity reduces abruptly from around 500°/sec to around 250°/sec.

14. Limitations and Future Refinements

The first implementation of the *VOR* model presented here is subject to certain limitations.

For example, a consequence of driving eye position from the RHP is that the model does not produce canal-driven torsion, because the fixation is a single point without orientation and our model adjusts only horizontal and vertical eye position to fixate upon it; "up" is always towards the top of the head. In future we expect to expand the model to incorporate the conceptual orientation of the fixation point. As rotation of the head is detected around the naso-occipital axis a filtered orientation of the fixation point could be maintained. We anticipate that this could usefully model canal-driven torsion.

In addition to head movement stimuli we expect to incorporate artificial vestibular stimuli, including caloric irrigation, galvanic stimulation and vibration. In order to accommodate these artificial stimuli we will separate gain and resting rate settings for each vestibular end organ into regular and irregular afferent populations so that stimuli and patient conditions can affect these independently (ie. galvanic stimulation will primarily activate and inhibit irregular afferents, patients with gentamicin ototoxicity will primarily lose regular afferent function, and patients with Ménière's disease may be better modelled with an increase in irregular gains). With this separation it will also be possible to model the jerk and acceleration components of natural motion stimuli such that they will primarily affect regular and irregular afferents respectively.

The ultimate object is that our model should predict responses to nearly all known vestibular stimuli.

15.Conclusion

The goal of the present thesis was to describe and implement a model of the processes that underlie the human vestibulo-ocular system. To the extent that the model successfully predicts many eye movement responses to known head movement stimuli under various known functional conditions, the model is valid. Whether or not the structures and processes described in the model actually have real-world analogous counterparts is unknown, and it is not the thesis of the present work that these structures and processes really exist; merely that the model produces physiologically plausible responses to a range or linear and angular motion profiles.

A summary of the model's predictions follows. The model predicts a simple first approximation of angular and linear VOR in normal subjects. This is the response that is easily observed to brief rotations and translations of the head.

Under conditions of constant rotation and head-relative fixation in darkness the model predicts the characteristic nystagmus that is caused by the subject's efforts to suppress VOR by generating catch-up saccades to the fixation target after the eye direction has been reflexively influenced by the VOR. After a period of constant rotation the model predicts that this nystagmus reduces and disappears as the response to constant velocity rotation decays, followed by a few nystagmus beats in the opposite direction. On deceleration of the subject to stationary the model predicts a similar sequence of post rotatory nystagmus and secondary nystagmus, decaying over some seconds.

During off-vertical axis rotation (OVAR) the eyes display nystagmus, which decays to a non-zero rate that is maintained indefinitely.

When the head is rotated at a constant velocity, then decelerated to stationary, followed immediately by a tilt around the naso-occipital axis, the secondary nystagmus rapidly disappears as the otolithic component of angular VOR overcomes the canal component.

The model predicts dynamic cyclovergence during vertical linear acceleration.

One of the benefits of preparing a model of this kind is that it can be used very simply to predict eye movement responses to stimuli and subject conditions that have not so far been tested or observed. It is hoped that researchers will explore the model and its predictions and seek to reproduce these in real human subjects. The degree to which the model's predictions match future real-world empirical observations will provide further support for the model. Conversely, when empirical observations disagree with the model's predictions this will provide evidence that the model is to some extent inaccurate or invalid. In this case it provides the opportunity to revise or update the model to incorporate the newly discovered observations.

16.References

Angelaki, D. E. (2004). Eyes on target: what neurons must do for the vestibuloocular reflex during linear motion. *Journal of Neurophysiology, 92*(1), 20-35.

Baloh, R., Honrubia, V., Yee, R., & Hess, K. (1984). Changes in the human vestibulo‐ocular reflex after loss of peripheral sensitivity. *Annals of neurology, 16*(2), 222-228.

Crane, B. T., Tian, J., Wiest, G., & Demer, J. L. (2003). Initiation of the human heave linear vestibulo-ocular reflex. *Experimental Brain Research, 148*(2), 247-255.

Curthoys, I. S., Wearne, S. L., Dai, M., Halmagyi, G. M., & Holden, J. R. (1992). Linear Acceleration Modulates the Nystagmus Induced by Angular Acceleration Stimulation of the Horizontal Canala. *Annals of the New York Academy of Sciences, 656*(1), 716-724.

Guedry, F. (1992). Perception of motion and position relative to the Earth: An overview. *Annals of the New York Academy of Sciences, 656*(1), 315-328.

Guedry, F. (1996). Spatial orientation perception and reflexive eye movements—A perspective, an overview, and some clinical implications. *Brain research bulletin, 40*(5), 505-512.

Halmagyi, G. M., & Curthoys, I. S. (1988). A Clinical Sign of Canal Paresis. *Archives of Neurology, 45*(7), 737-739.

Halmagyi, G. M., Curthoys, I. S., Todd, M. J., Dcruz, D. M., Cremer, P. D., Henderson, C. J., & Staples, M. J. (1991). Unilateral Vestibular Neurectomy in Man Causes a Severe Permanent Horizontal Vestibuloocular Reflex Deficit in Response to High-Acceleration Ampullofugal Stimulation. *Acta Oto-Laryngologica*, 411-414.

Harris, L. (1987). Vestibular and optokinetic eye movements evoked in the cat by rotation about a tilted axis. *Experimental Brain Research, 66*(3), 522-532.

Hixson, W. C., Niven, F. I., & Correia, M. J. (1966). Kinematics nomenclature for physiological accelerations with special reference to vestibular applications: DTIC Document.

Honrubia, V., Marco, J., Andrews, J., Minser, K., Yee, R. D., & Baloh, R. W. (1985). Vestibulo-ocular reflexes in peripheral labyrinthine lesions: III. Bilateral dysfunction. *American journal of otolaryngology, 6*(5), 342-352.

MacDougall, H. G., McGarvie, L. A., Halmagyi, G. M., Curthoys, I. S., & Weber, K. P. (2013). The Video Head Impulse Test (vHIT) Detects Vertical Semicircular Canal Dysfunction. *Plos One, 8*(4). doi: ARTN e61488 DOI 10.1371/journal.pone.0061488

MacDougall, H. G., Weber, K. P., McGarvie, L. A., Halmagyi, G. M., & Curthoys, I. S. (2009). The video head impulse test Diagnostic accuracy in peripheral vestibulopathy. *Neurology, 73*(14), 1134-1141. doi: Doi 10.1212/Wnl.0b013e3181bacf85

Niven, J. I., Hixson, W. C., & Correia, M. J. (1966). Elicitation of horizontal nystagmus by periodic linear acceleration. *Acta Oto-Laryngologica, 62*(1-6), 429-441.

Olasagasti, I., Bockisch, C., Zee, D., & Straumann, D. (2008). Cyclovergence evoked by up–down acceleration along longitudinal axis in humans. *Progress in brain research, 171*, 319-322.

Paige, G. D. (1983). Vestibuloocular reflex and its interactions with visual following mechanisms in the squirrel monkey. I. Response characteristics in normal animals. *J Neurophysiol, 49*(1), 134-151.

Ramat, S., Zee, D. S., & Minor, L. B. (2001). Translational Vestibulo‐Ocular Reflex Evoked by a "Head Heave" Stimulus. *Annals of the New York Academy of Sciences, 942*(1), 95-113.

Raphan, T., Matsuo, V., & Cohen, B. (1979). Velocity storage in the vestibulo-ocular reflex arc (VOR). *Experimental Brain Research, 35*(2), 229-248.

Viirre, E., Tweed, D., Milner, K., & Vilis, T. (1986). A Reexamination of the Gain of the Vestibuloocular Reflex. *Journal of Neurophysiology, 56*(2), 439-450.

Waespe, W., Cohen, B., & Raphan, T. (1985). Dynamic modification of the vestibulo-ocular reflex by the nodulus and uvula. *Science, 228*(4696), 199-202.

Weber, K. P., Aw, S. T., Todd, M. J., McGarvie, L. A., Curthoys, I. S., & Halmagyi, G. M. (2008). Head impulse test in unilateral vestibular loss - Vestibulo-ocular reflex and catch-up saccades. *Neurology, 70*(6), 454-463. doi: Doi 10.1212/01.Wnl.0000299117.48935.2e

Weber, K. P., Aw, S. T., Todd, M. J., McGarvie, L. A., Pratap, S., Curthoys, I. S., & Halmagyi, G. M. (2008). Inter-ocular differences of the horizontal vestibulo-ocular reflex during impulsive testing. *Using Eye Movements as an Experimental Probe of Brain Function - a Symposium in Honor of Jean Buttner-Ennever, 171*, 195-198. doi: Doi 10.1016/S0079-6123(08)00626-2

Wolfe, J. W., Engelken, E. J., & Kos, C. (1977). Low-frequency harmonic acceleration as a test of labyrinthine function: basic methods and illustrative cases. *Otolaryngology, 86*(1), ORL-130-142.

17.Appendix

The attached CD-ROM contains folders for each motion profile/condition combination described in the text. Each folder contains PDF files describing the respective motion profiles and conditions; PLIST files containing definitions of the motion profiles and conditions which can be imported into VOR via the iTunes File Sharing area; CSV files containing the data recorded during the profile; MOV files containing screen recordings of the 3D view and chart during the profile; and PNG files containing the charts recorded during the profiles.

01 Impulse LAT - 01 Normal - 20140909.1526

01 Impulse LAT - 02 UVL Left - 20140909.1530

01 Impulse LAT - 03 BVL - 20140909.1530

01 Impulse LAT - 04 Superior Neuritis Left - 20140909.1531

02 Impulse LAT close - 01 Normal - 20140909.1529

03 Impulse LARP - 01 Normal - 20140909.1611

03 Impulse LARP - 04 Superior Neuritis Left - 20140909.1531

05 Sinusoidal Yaw - 01 Normal - 20140909.1532

05 Sinusoidal Yaw - 02 UVL Left - 20140909.1532

05 Sinusoidal Yaw - 03 BVL - 20140909.1532

06 On-Centre Rotation - firing rates - 01 Normal - 20140909.1533

06 On-Centre Rotation - velocities - 01 Normal - 20140909.1536

07 Heave Y - 01 Normal - 20140909.1539

07 Heave Y - 02 UVL Left - 20140909.1539

07 Heave Y - 03 BVL - 20140909.1539

07 Heave Y - 05 Perfect - 20140909.1540

08 Oscillate Y - 01 Normal - 20140909.1541

08 Oscillate Y - 05 Perfect - 20140909.1541

09 Oscillate Z - 01 Normal - 20140909.1542

10 Oscillate X - 01 Normal - 20140909.1543

11 Linear Sled Y - 01 Normal - 20140910.1049

12 Centrifugation Forward - 01 Normal - 20140909.1544

13 Centrifugation Backward - 01 Normal - 20140909.1546

14 OVAR - 01 Normal - 20140909.1549

15 Tilt Dump - 01 Normal - 20140909.1551